

USING VCOS AS RF MEASURING DEVICES

by

Carl Elliot Taylor

BS, University of Pittsburgh, 2000

Submitted to the Graduate Faculty of
the University of Pittsburgh in partial fulfillment
of the requirements for the degree of
Master's of Science in Electrical Engineering

University of Pittsburgh

2004

UNIVERSITY OF PITTSBURGH

SCHOOL OF ENGINEERING

This thesis was presented

by

Carl Elliot Taylor

It was defended on

August 4th, 2003

and approved by

James T. Cain, Assistant Professor, Electrical Engineering Department

Raymond R. Hoare, Assistant Professor, Electrical Engineering Department

Ronald G. Hoelzeman, Assistant Professor, Electrical Engineering Department

Thesis Advisor: Marlin H. Mickle, Nickolas A. DeCecco Professor, Electrical Engineering Department

USING VCOS AS RF MEASURING DEVICES

Carl Elliot Taylor, MS

University of Pittsburgh, 2004

This thesis presents an alternative way to test the amount of energy harvested by an antenna. Accurately measuring the amount of energy an antenna harvests is a challenge. The test equipment that touches the antenna can greatly affect the results of the test. Using a VCO to measure an antenna's harvested power enables accuracy and prevents the need to attach testing equipment. The VCO is powered by a harvesting antenna. The frequency produced is then output to a transmitting antenna. The output frequency of the VCO can easily be determined and then used to look up the power from the characteristics of the VCO. A background study of types of VCOs, and VCOs available on the market will also be included in this thesis. Finally the experiment setups and results will be presented.

TABLE OF CONTENTS

1.0 BACKGROUND OF THE PROBLEM.....	1
1.1 GENERALITIES	1
1.2 STATEMENT OF THE PROBLEM.....	2
2.0 ANTENNAS ON-CHIP	3
2.1 RF ID TAGS.....	4
2.1.1 On-Chip Solution.....	4
2.1.1.1 Antennas	7
3.0 CURRENT ANTENNA TESTING PROBLEMS.....	10
3.1 CONNECTED TEST EQUIPMENT.....	10
3.2 LED POWER METER	11
4.0 BACKGROUND OF A VCO.....	14
4.1 VCO DEFINITION	14
4.2 TYPES OF VCOS.....	17
4.2.1 LC Oscillators	18
4.2.2 Non-LC Oscillators.....	19
4.2.2.1 Current Starved Oscillator	20
4.2.2.2 Interpolation.....	23
4.2.3 Special Components.....	24
4.2.3.1 Tunable Capacitors	25
4.2.3.2 Tunable Diode.....	29
4.2.3.3 Varactor Transistors.....	30
5.0 CURRENT VCO USES.....	35
5.1 PHASE LOCK LOOPS	35
6.0 THE VCO SOLUTION	37
7.0 ANALOG SUPPORT CIRCUITRY.....	38

7.1 SPIRAL DELTA ANTENNA	39
7.2 CHARGE PUMP	40
7.3 IMPEDENCE MATCHING	41
7.4 AMPLIFIER	42
8.0 AVAILABLE TECHNOLOGIES	44
9.0 THE VCO DESIGN AND VERIFICATION EXPERIEMENTS	46
9.1 OSCILATOR DESIGN	46
9.1.1 Experiment Description	46
9.1.1.1 Objective	46
9.1.1.2 Background Information	47
9.1.1.3 Test Setup	51
9.1.2 Results	62
9.1.2.1 VCO 1 Results	63
9.2 TRANSMISSION I EXPERIMENT	67
9.2.1 Description	67
9.2.1.1 Objective	67
9.2.1.2 What was accomplished	68
9.2.1.3 Test Rig Setup	69
9.2.1.4 Equipment Setup	72
9.2.2 Results	75
9.3 TRANSMISSION II EXPERIMENT	77
9.3.1 Description	77
9.3.1.1 Objective	77
9.3.1.2 What was accomplished	77
9.3.1.3 Test Rig Setup	78
10.0 CONCLUSION	81
11.0 CONTRBUTIONS	82
APPENDIX A	84
VCO Comparison Test	84
11.1 VCO 1 Results	84
11.2 VCO 2 Results	87

APENDIX B	90
Transmission Experiment	90
11.3 Transmission Results	90
BIBLIOGRAPHY	93

LIST OF TABLES

Table 1. LED Power Look Up Table	12
Table 2. VCO1 (digital) Analyzer Results.....	64
Table 3. VCO2 (analog) Analyzer Results	65
Table 4. Transmitted Results Compared to the Non-Transmitted Results	76

LIST OF FIGURES

Figure 1. E-ZPass Electric Toll Collector.....	5
Figure 2. Mobil's Speedpass ID Tag	6
Figure 3. An On-Chip, Self-Contained RF-ID.....	7
Figure 4. RF-ID Block Diagram	8
Figure 5. LED Power Meter.....	12
Figure 6. Frequency vs. Voltage of an Ideal VCO	15
Figure 7. Tuning Non-Linearity.....	17
Figure 8. CMOS oscillator with self-switching inductors	19
Figure 9. Ring Oscillator.....	20
Figure 10. A Full Current Starved VCO	21
Figure 11. A Simple Current-Starving Circuitry	22
Figure 12. Current Starved Ring Oscillator	23
Figure 13. Interpolation Node Ring.....	23
Figure 14. Interpolation Node.....	24
Figure 15. A Simplified Colpitts Oscillator.....	25
Figure 16. A Negative Resistance LC Oscillator.....	26
Figure 17. Varactor Capacitor Conceptual	27
Figure 18. Varactor Capacitor Profile.....	28
Figure 19. VCO Containing Varactor Capacitors.....	29
Figure 20. Topology of VCO with a Tunable Diode	30
Figure 21. VCO with PMOS Capacitors.....	31
Figure 22. Varactor Transistor with $B = D = S$	32
Figure 23. An A-MOS Varactor Transistor Profile	33
Figure 24. A-MOS vs. $B=D=S$	33
Figure 25. Phase-Locked-Loop Block Diagram	36

Figure 26. Support Circuitry Flow Chart.....	39
Figure 27. The Spiral Delta Antenna	40
Figure 28. Voltage Doubler	41
Figure 29. Voltage Doubler Layout.....	41
Figure 30. A Simple π Matching Network.....	42
Figure 31. Low Noise Amplifier.....	43
Figure 32. Current Starved Oscillator with Sizes	49
Figure 33. APLAC's Oscillation Simulator.....	50
Figure 34. Ansoft's Oscillator Simulator.....	51
Figure 35. VCO Chip with the Patch Antennas.....	52
Figure 36. Example of a Circuit Using a Mirroring Technique.....	53
Figure 37. Dummy elements outside of the protected elements.....	54
Figure 38. An example of using unit sizes.....	54
Figure 39. An example of a guard ring.....	55
Figure 40. An example of a capacitor using the finger technique	56
Figure 41. Digital Style VCO layout (VCO1)	57
Figure 42. Analog Style VCO layout (VCO2).....	58
Figure 43. The VCO Test Rig.....	59
Figure 44. Theta Wire Bonds.....	60
Figure 45. Pomona 3073 Power Adaptor.....	61
Figure 46. Power Supply.....	61
Figure 47. VCO Test Setup.....	62
Figure 48. VCO1 and VCO2 Frequency vs. Voltage	66
Figure 49. VCO1 and VCO2 dBm vs. Voltage	66
Figure 50. Theta chip	69
Figure 51. Epsilon Chip	70
Figure 52. Test Rig	71
Figure 53. Bonding Diagram of Transmission Experiment.....	72
Figure 54. Test Equipment.....	73
Figure 55. Maxrad 900 MHz antenna	73
Figure 56. Spectrum Analyzer, Test Rig and Receiving Antenna.....	74

Figure 57. Transmit I Test Setup	75
Figure 58. Transmitted I Compared to Non-Transmitted Results	76
Figure 59. Iota Chip	78
Figure 60. Bonding Diagram of Transmission II Experiment	79
Figure 61. Transmitting II Test Setup.....	80
Figure 62. VCO 1 Analyzer Results: 1.5 Volts and 2.0 Volts	84
Figure 63. VCO 1 Analyzer Results: 2.5 Volts and 3 Volts	85
Figure 64. VCO 1 Analyzer Results: 3.5 Volts and 4 Volts	85
Figure 65. VCO 1 Analyzer Results: 4.5 Volts and 5 Volts	86
Figure 66. VCO 1 Analyzer Results: 5.5 Volts and 6 Volts	86
Figure 67. VCO 2 Analyzer Results: 1.5 Volts and 2 Volts	87
Figure 68. VCO 2 Analyzer Results: 2.5 Volts and 3 Volts	87
Figure 69. VCO 2 Analyzer Results: 3.5 Volts and 4 Volts	88
Figure 70. VCO 2 Analyzer Results: 4.5 Volts and 5 Volts	88
Figure 71. VCO 2 Analyzer Results: 5.5 Volts and 6 Volts	89
Figure 72. Transmitted Analyzer Results: 2.5 Volts and 3 Volts	90
Figure 73. Transmitted Analyzer Results: 3.5 Volts and 4 Volts	91
Figure 74. Transmitted Analyzer Results: 4.5 Volts and 5 Volts	91
Figure 75. Transmitted Analyzer Results: 5.5 Volts and 6 Volts	92

ACKNOWLEDGEMENTS

First of all I would like to thank Dr. Marlin Mickle for his support and guidance. He has been a big part of my success with my experiments, my thesis, and mentoring me. I would like to thank Dr. Thomas Cain, Dr. Ronald Hoelzeman, and Dr. Hoare for their advice and sitting on my thesis committee. I would like to thank Dr. Minhong Mi for his information on the voltage doubler. I would like to thank Charlie Greene for his advice on the impedance matching. I would also like to thank Dr. Frank Herzel who was very helpful when I requested more details about a VCO that was in one of his papers [1].

1.0 BACKGROUND OF THE PROBLEM

1.1 GENERALITIES

Wireless electronic devices continue to become smaller and smaller. As this transition of design and development progress, it becomes more and more difficult to fabricate and test these prototype wireless devices and their chip (die) implementations. Any physical connection to the device under test (DUT) tends to distort the RF profile of the DUT.

While many proposed techniques may solve problems of this type, for example, simulation, the critical questions of the functionality can only be answered by building a prototype of the device. The solution for the wireless prototype is to fabricate an integral wireless element(s) that will transmit various parameter measurements as data on a wireless communication link. There are various technologies such as radio frequency (RF) and infrared (IR) to facilitate the wireless transmission.

This thesis primarily focuses on research to implement a parametric data link using RF. In the category of RF, the link will transmit coded data through modulating a carrier frequency, varying the frequency to denote parametric values of voltage that can provide energy and power.

The designing of the CMOS devices and implementing a wireless link that uses frequency as the basis for transmitting parameter values will also be the focus of this thesis. The parameter measurements will be in the terms of DC voltages, and the transducer (voltage to frequency) will be a voltage controlled oscillator (VCO).

1.2 STATEMENT OF THE PROBLEM

The problem to be solved is the design, testing and evaluation of a voltage controlled oscillator (VCO) in CMOS for use in the measurement of power harvested on autonomous operating without batteries and wireless chips. The research will consider alternative topologies and CMOS layouts. The VCO will be tested by transmission through an antenna to a receiving antenna connected to a spectrum analyzer. The context and basis for the evaluation of alternative VCO implementations will also be presented.

2.0 ANTENNAS ON-CHIP

An emerging field that has sparked the interest of many is the study of on-chip antennas. Until recently radio frequency (RF) transmissions have been limited to macro antenna designs, which are on the order of several square inches. The ability to make an antenna of the micro size is extremely valuable due to reductions in cost and the method of attaching the antenna to products. There are many uses for such a device.

The current commercial antennas are not on the same chip with the rest of the circuitry and require wire bonding or other methods of precision attachment. This is an expensive, time consuming step in manufacturing. Having an antenna on the chip reduces the cost of the circuit drastically. It can also be fabricated at the same time with the other devices on the chip.

Isolating a circuit from the outside environment is another growing interest. A chip that does not need batteries or wires attached to it makes this possible. This enables it to be used in environments where outside bacteria or particles must not come in contact with it. It also can be embedded making wireless communication possible in demanding environments.

The market for an on-chip antenna is overwhelming. The number of applications is too large to determine based on current concepts. The most popular application is an identification tag. The tags can be used to track anything from products in a warehouse to instruments in an emergency room.

2.1 RF ID TAGS

An RFID tag is the fundamental device in an identification technology based on electronic waves. It has an advantage over the bar code system because no contact or orientation is needed, it can read and store data, and it can achieve a large amount of information capacity [18].

The potential for affordable RFID tags is enormous. They can revolutionize many industries. A few of the industries that it would greatly affected by the tags is the retail market, Electric Toll Collection (ETC), medical, and warehouse inventory.

Shopping markets as well as other retail stores can use the tag instead of a traditional bar code. The tag would speed shopping checkout lines drastically. It would also allow automatic inventory updates. A product can be tracked from its creation, to the warehouse, to the unloading from the truck, to the shelf on the store, and through the checkout as well as providing a capability for essentially instant inventory.

An example of the potential of an RFID tag is the current ETC system, E-ZPass. E-ZPass, an electronic toll payment system, is available in many north eastern states. This lowers the number of toll attendants required, and greatly speeds up the flow of traffic.

The tags also improve automatic payment systems like Mobil's Speedpass. The tag is about an inch long and is worn on a key ring. This tag makes it fast and convenient to pay for your gas without having to go inside or having to insert a credit card into the machine. This technology can also be extended to parking meters, or any other type of purchase.

2.1.1 On-Chip Solution

In order for RFID tags replace the bar code and become the retail standard, the manufacturing cost of the tags must be greatly reduced. There are two changes that can take place to make the

tags affordable. The antennas can be placed on the chip with the rest of the circuitry, and the size of the tag needs to be greatly reduced.

A self-contained chip would exhibit the largest reduction in cost. The key to a self-contained chip is to have multiple antennas on the tag. These antennas are used for harvesting energy and transmitting the identification information.

Reducing the size of the chip is the next challenge. The smaller the design, the more chips that can be produced from a single fabrication run. As the number of chips produced on a single run increases, the price of the chips decreases. This is essential to get an ID tag down to the “ultimate” target price of 1 cent.

E-ZPass devices for example are the size of a cassette tape. These tags are free to the user, but cost the E-ZPass service roughly \$2.00 to manufacture [20]. The tags could cost less than 10 cents. The savings in the tag production could be passed on to the customers or improving the road system. Figure 1 is a picture of the current E-ZPass tag.



Figure 1. E-ZPass Electric Toll Collector

The cost of the current tags, like Speedpass, is roughly 75 cents or more. Inside the tag's casing is an antenna, a chip containing identification information and wire that connects them. The antenna and the chip can be manufactured inexpensively, but the process required to connect them is costly and time consuming. That is the most expensive step of the process.

Having a self-contained, on-chip solution cuts the cost to a fraction. The antennas can be on the chip with the identification hardware. This step will drastically reduce the size of the tag, and cut out the costly bonding from the antenna to the chip. The same Speedpass tag (shown in figure 2) may be only 2mm in length as apposed to 25mm.



Figure 2. Mobil's Speedpass ID Tag

The chip does not need batteries, or need to be visually seen so that it can be embedded, or coated. That is the advantage that makes these tags extremely useful in the retail market, medical fields, and many more. Below in figure 3 is a self contained ID tag and its block diagram in figure 4.

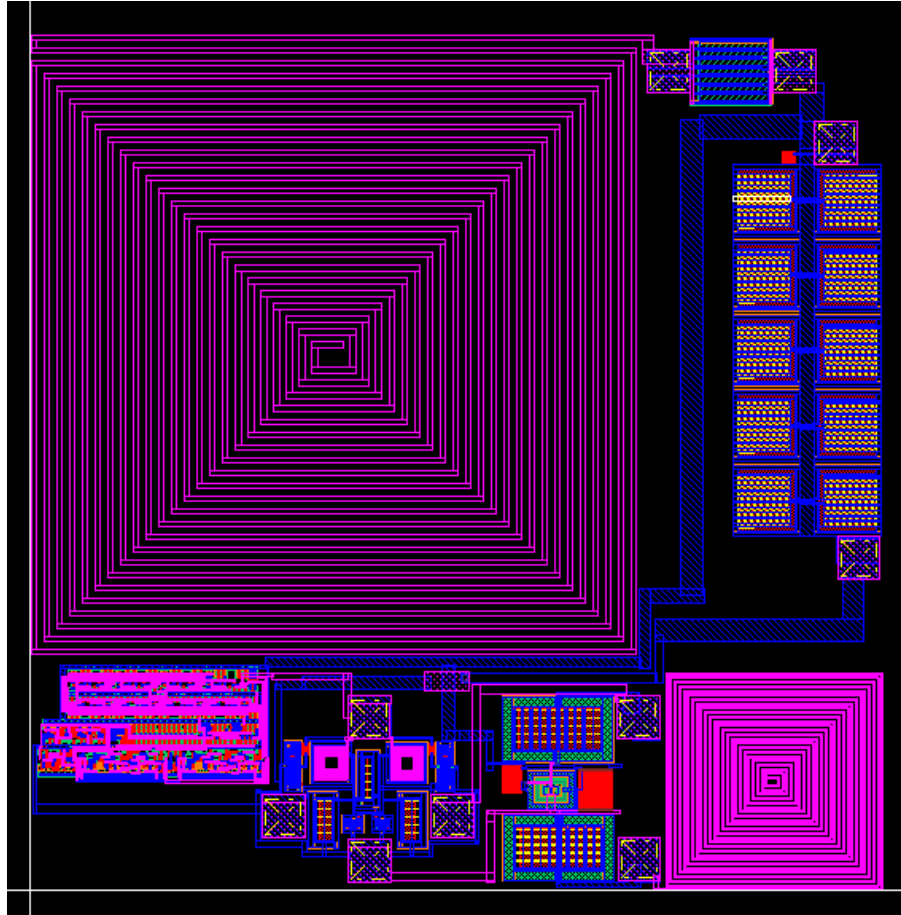


Figure 3. An On-Chip, Self-Contained RF-ID

2.1.1.1 Antennas

An essential component of an RFID tag is the antenna. The quality of the antenna will determine the tag's operating range, the orientation in which it will operate, and the amount of power it can supply to the electronics.

Up to three antennas can be used in RFID tags, which are energy harvesting, transmitting, and receiving. Energy harvesting is the key to powering the chip. The second antenna is the transmitting antenna. The third antenna, the receiving antenna, is not required for a typical ID tag. This antenna is used to change the output transmission.

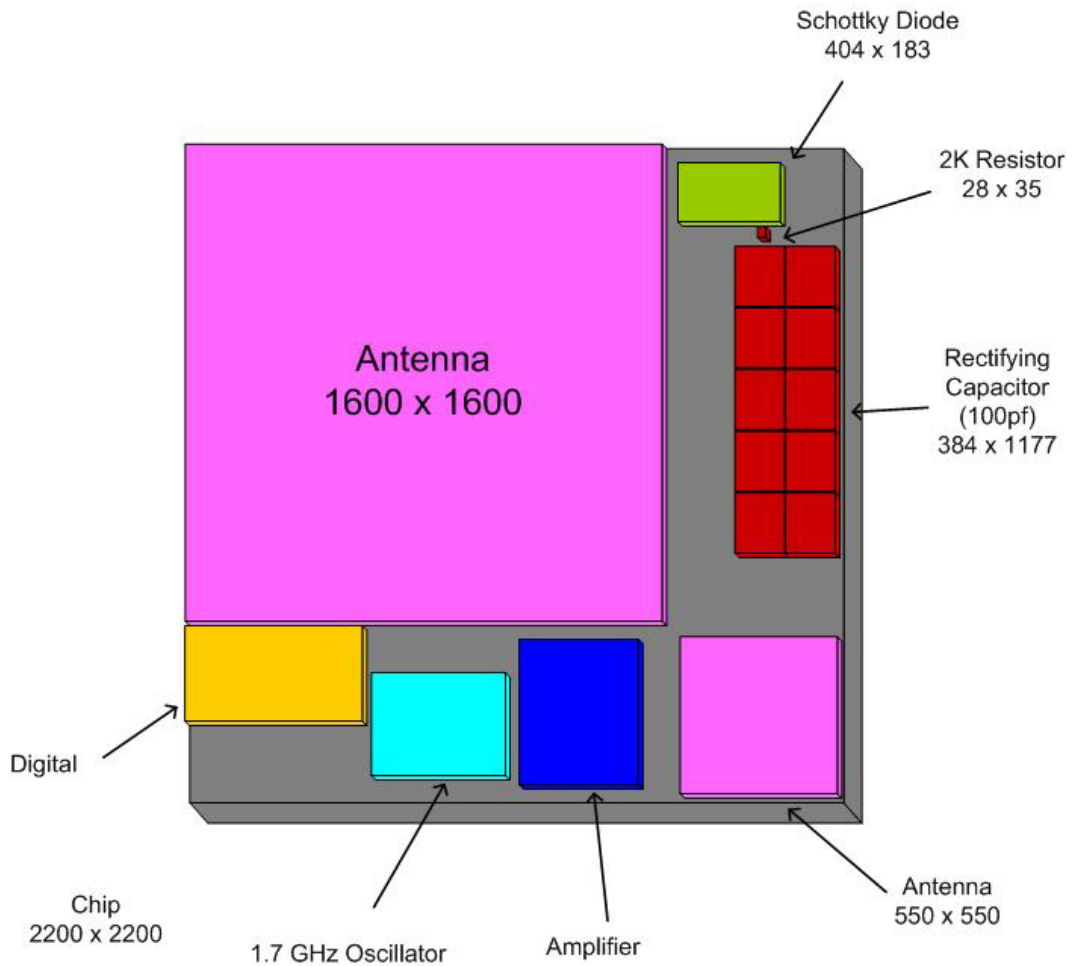


Figure 4. RF-ID Block Diagram

Energy Harvesting

Energy harvesting allows low power circuits that traditionally require batteries or solar power as a power source to operate without either. The antenna is used to harvest RF energy out of the air so it can be converted into usable energy. The capability to harvest energy allows the tag to have numerous uses as well as being an essential part of a RFID tag.

Transmitting

The transmitting antenna sends the tag's identification to a receiving device. This antenna is typically tuned to a different frequency than the energy harvesting and receiving antennas. The transmitting antenna input voltage signal must typically be amplified. The quality of the antenna and the matching network determines the transmitted signal strength. Strong signal strength can help reduce the cost of the reading equipment.

Receiving

An additional receiving antenna can be used to select multiple outputs. Two outputs can be hard-coded on the chip and the receiving antenna would select one of the two. The third antenna can also be used to program the chip. A series of bits can be sent to the chip through the antenna and stored. When the chip is activated, the stored bits are transmitted.

Having multiple antennas on the same chip complicates the design and testing drastically. Each antenna must operate at a different frequency. The different frequencies on a single chip can cause unwanted noise, which can affect the efficiency of the other antennas. Also, the goal is to reduce the size of the chip and adding another antenna will make it much larger. Therefore designs that require a third antenna are avoided if possible.

3.0 CURRENT ANTENNA TESTING PROBLEMS

The increasing demand for on-chip antennas is alarming. The design of antennas is very challenging due to the complexity of antenna theory and the effect the surrounding environment has on an antenna. Moving to the micro size when designing antennas on chips is even more challenging. The parasitics from the other devices that are also on the chip affect an antenna's behavior as well as the chip's environment.

Testing an antenna's efficiency has been a major hurdle in their development. When test equipment is connected to the antenna the equipment can become an antenna itself. Differentiating the antenna and surrounding circuitry can become extremely involved. A convenient method of testing is needed that does not touch the actual chip.

3.1 CONNECTED TEST EQUIPMENT

The traditional method of testing an energy harvesting antenna is to expose it to RF energy and to measure the results with a connected oscilloscope, while shielding the wire as much as possible.

This method typically involves wire bonding the output of the antenna to typically an SMA connector, and connecting coaxial cable, which is attached to say a spectrum analyzer. This solution causes three major problems. The first problem is the coaxial cable can inject noise, or feedback into the circuit, which may be difficult to determine.

The second problem is the connecting cable, as well as the wire bond can become an antenna. It is not possible to shield the wire bond, and even with the cable shielding the RF waves can bounce around the shield and contaminate the results.

The third problem is that the wire attached to the chip may make it hard to change the orientation of the chip to check transmission at different angles. The current primary purpose of the chip is to replace the bar code. Therefore the chip must be able to transmit and receive in any orientation. The ability to test without the test equipment being required to touch the chip will greatly simplify this task.

3.2 LED POWER METER

Another one of the previous methods that we used to test energy harvesting antennas was the LED power meter. The power meter is also not very practical for testing on-chip antennas and was not precise. The LED power meter (figure 5) uses LEDs to estimate the amount of power the antenna is harvesting. The columns of lights illuminated indicates different amount of voltage and the intensity indicates the amount of power harvested. Table 1 lists the LEDs corresponding to a given voltage.

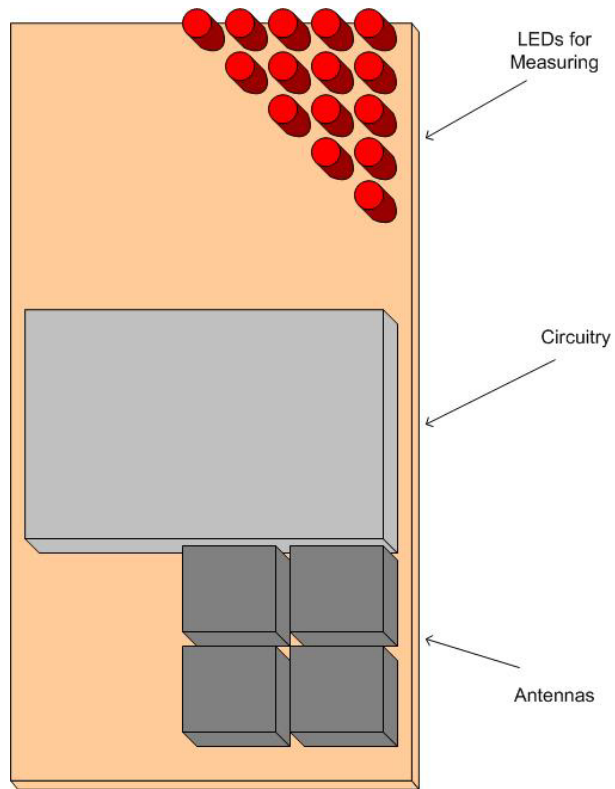


Figure 5. LED Power Meter

Table 1. LED Power Look Up Table

LED Power Meter		
Column	Voltage (V)	Power (mW)
One:	1.8	0.09
Two:	3.5	4.03
Three:	5.3	18.23
Four:	7.0	46.40
Five:	8.8	97.42
all LED's:	12.0	252.00

The key reason for the lack of precision of the LED Power Meter is not being able to determine intermediate voltages when certain LEDs are illuminated. The LED may receive a current insufficient to completely illuminate it. Determining which LEDs are completely lit and which LEDs are partially lit becomes difficult. Therefore, the amount of illumination must be estimated, and the power corresponding to partially illuminated LED must also be estimated. This problem was the reason for a need for an alternative method of antenna testing. In addition, this method was used for printed circuit boards (PCB) implementations and is not practical for CMOS chip fabrications.

4.0 BACKGROUND OF A VCO

Before the new method of testing antennas is discussed, some background information on Voltage Controlled Oscillators (VCOs) is necessary. As well as giving a brief description of what a VCO is, a number of topologies will be presented along with their advantages and disadvantages.

4.1 VCO DEFINITION

A Voltage Controlled Oscillator (VCO) is a device that produces alternating current whose frequency varies as a function of a DC voltage or current. The output frequency is altered by changing the control voltage or current. An ideal VCO has a linear change in the output frequency as the voltage changes linearly.

The gain (K_{vco}) or sensitivity of a VCO is defined in equation 1.1. The gain is the slope of the frequency change over the voltage change [3].

$$K_{vco} = \frac{f_{\max} - f_{\min}}{V_{\max} - V_{\min}} \text{ (Equation 1.1)}$$

The output frequency of a VCO is noted as ω_{out} , which is defined in equation 1.2. V_{cont} is the control voltage, and ω_0 is the frequency when the control voltage is zero (if an oscillation is still possible at zero). Figure 6 visually defines both K_{vco} , ω_0 and ω_{out} .

$$\omega_{out} = \omega_o + K_{vco} \cdot V_{cont} \quad (\text{Equation 1.2})$$

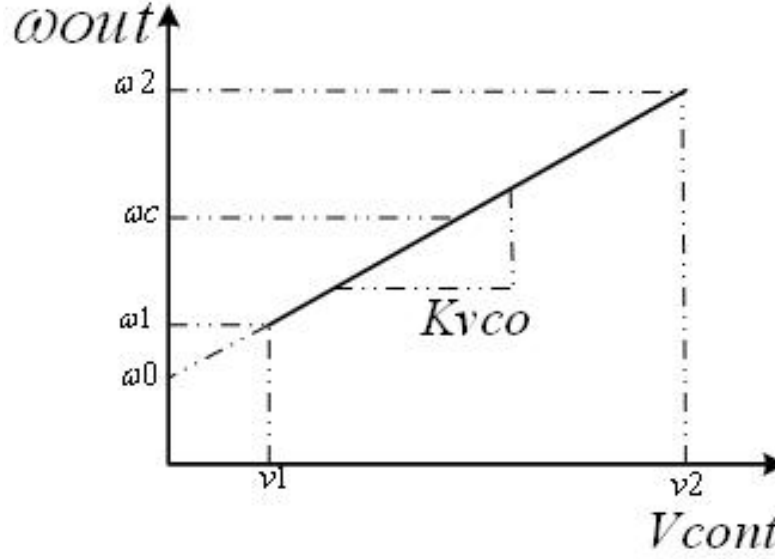


Figure 6. Frequency vs. Voltage of an Ideal VCO

The different performance parameters that distinguish one VCO from another are the following: center frequency, tuning range, lock range, tuning linearity, output amplitude, power dissipation, and signal output noise.

The center frequency (ω_c) is the frequency in the middle of the maximum and minimum frequencies of the VCO, as shown in equation 1.3. ω_2 is the highest frequency and ω_1 is the lowest frequency at which the VCO will oscillate. The operating temperature will also affect the center frequency [3].

$$\omega_c = \frac{\omega_2 - \omega_1}{2} \quad (\text{Equation 1.3})$$

The tuning range ($\omega_2 - \omega_1$) is determined by the minimum and maximum frequency swing when the control voltage is changed. Due to the potential change in center frequency because of a change in operating temperature, it is recommended to design the tuning range to be larger than required [3].

The lock of a circuit is the ability of the oscillator to continue to oscillate. Lock range is the range in which the input frequency may be changed before the loop loses its lock or stability. This is important because it is used to determine the size of the components in the tank circuit typically used for oscillations [4].

Tuning non-linearity is encountered when K_{vco} is not constant. This is a negative effect which causes inconsistency throughout the tuning range. It is desirable to minimize the variation of K_{vco} . Typically the gain, K_{vco} of an oscillator is greater around its center frequency. This characteristic leads to greater sensitivity in certain sections of the frequency range [3]. An example of this is in figure 7.

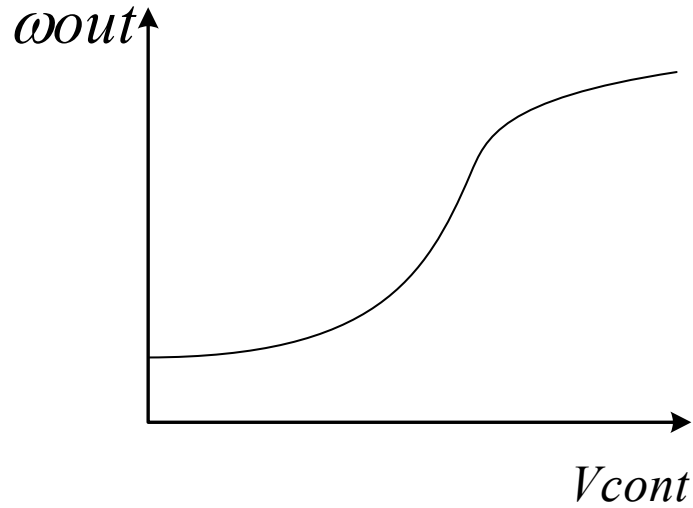


Figure 7. Tuning Non-Linearity

The output signal quality is the signal to noise ratio. It also is the quality of the actual oscillation. The quality of the oscillation is the consistency of the oscillation at a given frequency. Even with a consistent control voltage the oscillation frequency can vary. The noise of the components in the oscillator can cause these effects. Components with high Q values are required to raise the signal to noise ratio, and the quality of the overall oscillation.

4.2 TYPES OF VCOS

There are typically three types of voltage controlled oscillators; (1) the traditional (inductor/capacitance) LC oscillator, (2) the non-LC oscillator, and (3) oscillators containing special components making variable oscillation possible. The two oscillators with the special components discussed in this thesis contain electromechanically tunable capacitors, and MOS varactor transistors.

4.2.1 LC Oscillators

The traditional LC VCOs are the most popular for a number of reasons. They do not require a special, expensive fabrication process, unlike some of the electromechanically tunable capacitors or varactor transistors. The signal to noise ratio is typically higher than that of a phase lock loop. The Q values achieved by LC oscillators are superior to the other types of oscillators in the quality for the amount of design effort and cost of fabrication. They also do not require an external clock signal.

The oscillation is created from negative feedback which causes the circuit to be unstable. The instability eventually causes a phase shift. When the V_{cont} is changed on a traditional VCO the amount of negative feedback is proportionally changed. The result is an output frequency that varies [6]. The tuning range is typically smaller compared to the other types of oscillators.

Efforts have been directed towards improving the width of the tuning ranges without having to use varactor elements or non-LC circuitry. Using inductors in parallel can achieve both high Q values, and wide tuning ranges, like the circuit in figure 8. Transistors M1 and M2 when turned on cause L1 and L2 to be in parallel, which lowers the inductance of the tank. The result of the inductance being lower is the frequency is high. When V_{cont} is lowered, the current through L2 is lowered, therefore lowering its inductance. V_{cont} eventually reaches zero and all of the current flows through L1 [23]. The inductance across L1 is increased and the frequency will decrease.

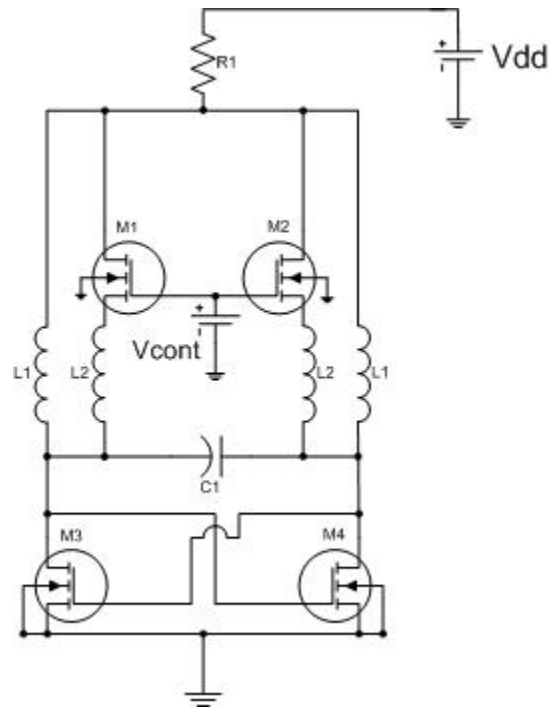


Figure 8. CMOS oscillator with self-switching inductors

4.2.2 Non-LC Oscillators

The non-LC oscillators have characteristics similar to a digital circuit. They behave like an analog circuit, but have similar characteristics to that of a digital design. There are two types of non-LC VCOs. The first is the current starved oscillator, and the second is a technique called interpolation.

The advantage of the non-LC Oscillators is their wide tuning range. Their tuning range can be as large as three times the tuning range of the LC VCOs. They also are easy to design. These two properties make them popular. The disadvantage the non-LC oscillators have is the relatively high phase noise. This is due to the circuit not containing any passive resonant elements [21].

4.2.2.1 Current Starved Oscillator

The most basic of these circuits is the current-starved CMOS inverter. This is based on a simple CMOS ring oscillator (figure 9).

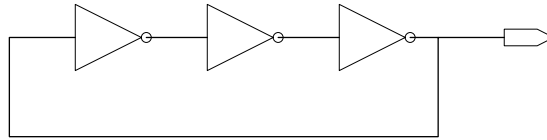


Figure 9. Ring Oscillator

The ring of inverters results in no stable DC points throughout the circuit. The logic level propagates around the loop, causing one inversion each time through the loop.

The oscillation period for a ring oscillator is twice the propagation delay:

$$f_{osc} = \frac{1}{2n \cdot T_{pd}} \quad (\text{Equation 1.3}).$$

n is the number of inverters in the ring (n must be an odd number to insure the sign of the feedback), and T_{pd} is the propagation delay.

In order to convert a ring oscillator into a VCO, the total propagation delay must be changed. There are two ways to do this, varying the load, or varying the current drive of the inverters. Adjusting the current causes the effective propagation delay of the inverters to be changed, which changes the frequency of the circuit [4]. Figure 10 is an example of a current starved topology.

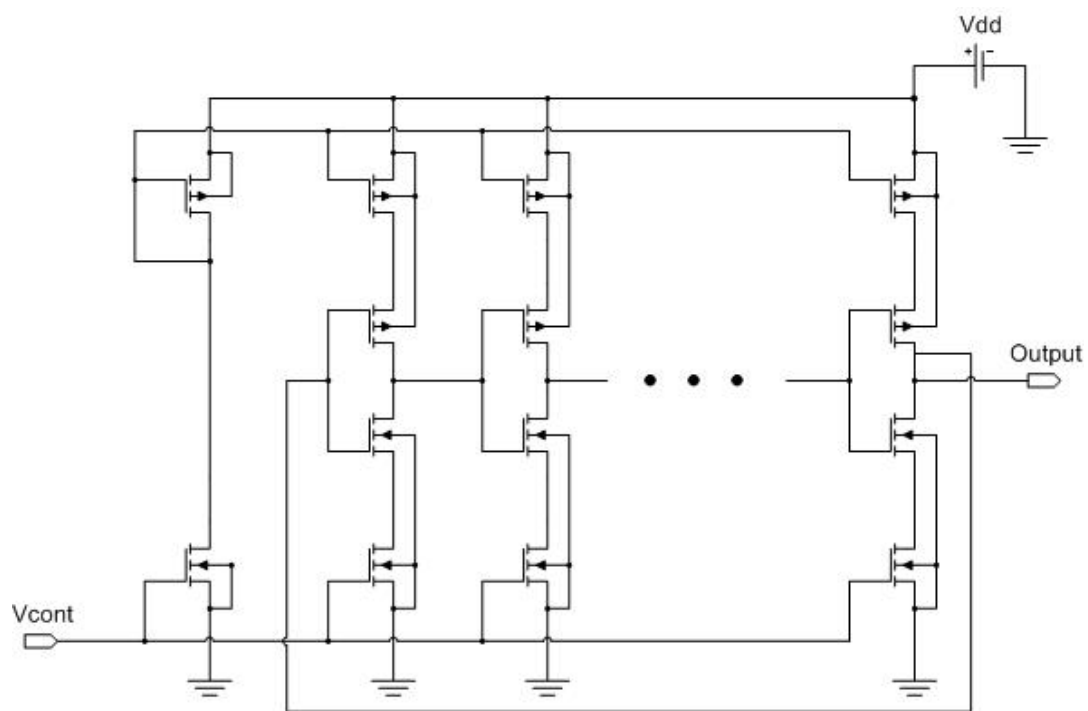


Figure 10. A Full Current Starved VCO

Other Current Starved Topologies

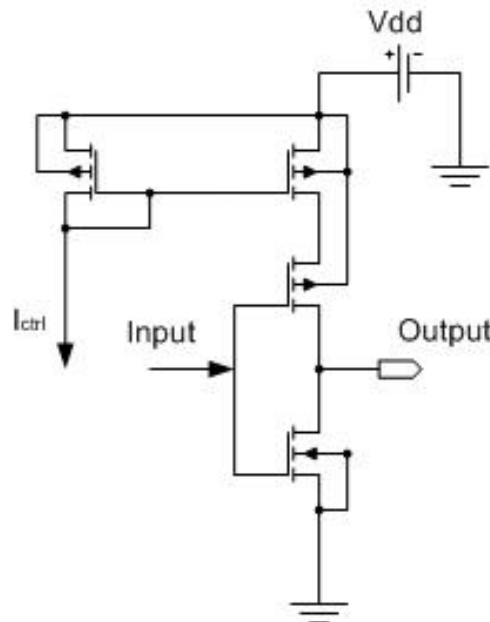


Figure 11. A Simple Current-Starving Circuitry

The VCO in figure 12 is a basic ring oscillator with three inverters forming the ring. The transistor that changes the amount current that flows through the ring is the NMOS transistor that has V_{cont} as an input into the gate. When V_{cont} is at V_{dd} , the full current is able to flow to the ring oscillator. As the voltage is lowered, the current through the ring oscillator is limited. The buffer at the end of the circuit pulls the signal back up to V_{dd} .

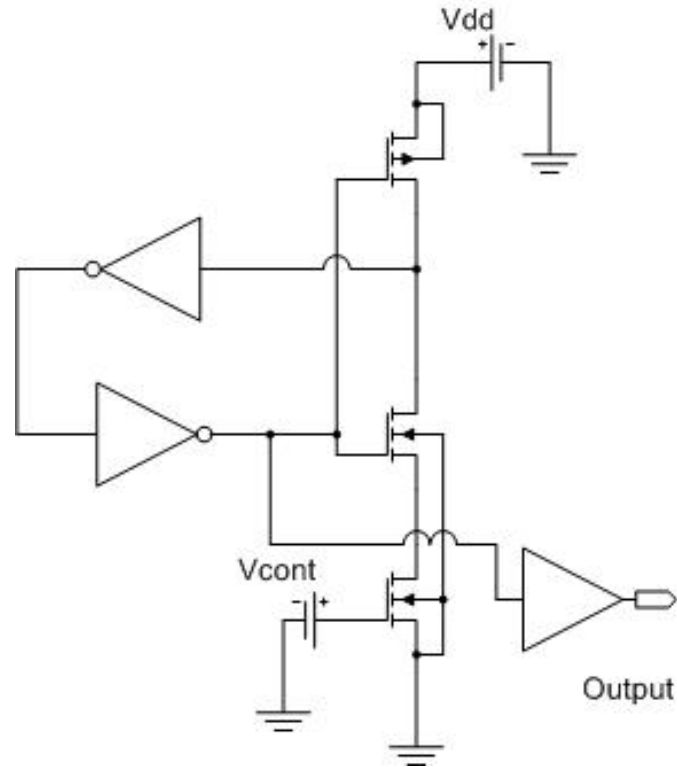


Figure 12. Current Starved Ring Oscillator

4.2.2.2 Interpolation

Another technique to tune ring oscillators is interpolation. Simple adjustable nodes are inserted into a traditional ring oscillator to accomplish this (figure 13).

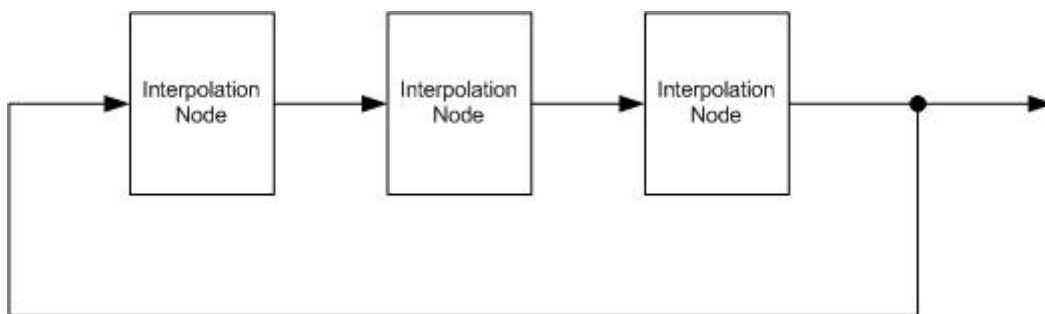


Figure 13. Interpolation Node Ring

The node (figure 14) has two tracks in which the current can follow. The control voltage V_{cont} turns each track on and off. The node is a current adder, which can just be a basic current mirror. A current mirror is based on copying a current from a reference. That requires that a precisely defined current source is already available [3].

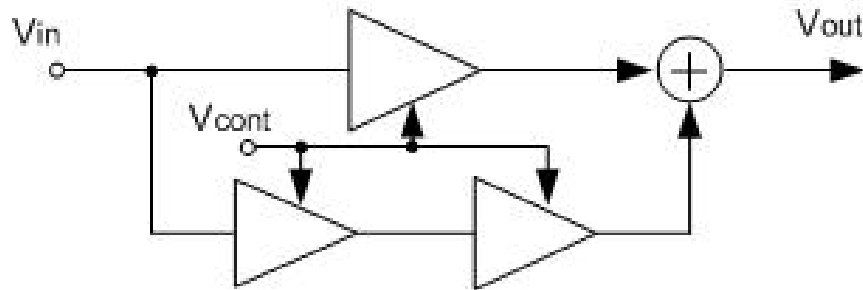


Figure 14. Interpolation Node

4.2.3 Special Components

Another method of creating a VCO is to use a traditional oscillator topology and electrically alter the properties of the components. This technique makes it possible to build a complex circuit with a simple topology. It also has the capability of producing extremely high Q values.

The special components often require special fabrication processes or post-fabrication alterations. Some however do not require a special fabrication process, but do require changes to the technology files of the CAD tools. The CAD tools prevent certain masks from being placed near or on other masks assuming that the user has made an error. Turning off those errors makes it possible to create some of these components in a traditional CMOS process.

4.2.3.1 Tunable Capacitors

A traditional oscillator that contains micromachined electromechanically tunable capacitors is a new, experimental type of VCO. The tunable capacitors are an integral part of this design. A VCO can be realized from the very basic oscillator topologies. One of the most basic topologies is the Colpitts oscillator in figure 15.

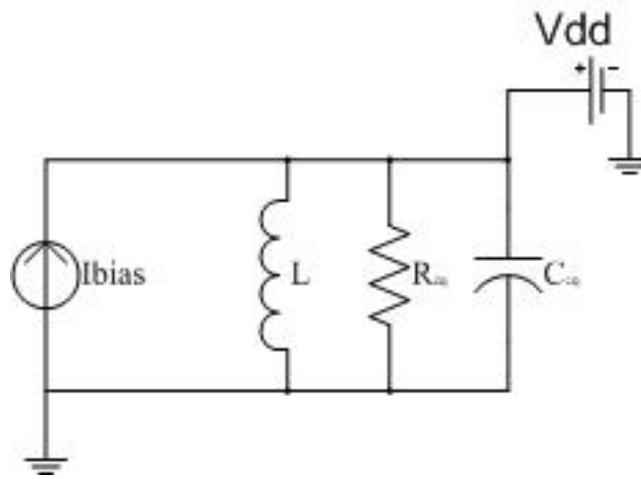


Figure 15. A Simplified Colpitts Oscillator

The frequency of a traditional Colpitts LC oscillator is:

$$f = \frac{1}{\sqrt{LC}} \text{ (Equation 1.4).}$$

Another popular, simple topology is the negative resistance LC oscillator, which is shown in figure 16. The negative resistance that is formed in the tank makes this topology popular. The negative resistance guarantees an oscillation will occur when noise is injected into the circuit. Tapped resonators are added to a basic negative resistance LC oscillator to achieve signal amplitudes above the available supply or breakdown voltages [4].

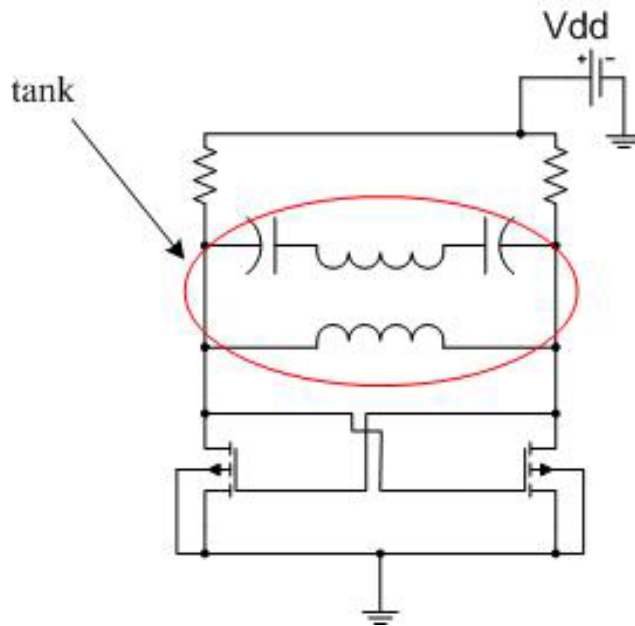


Figure 16. A Negative Resistance LC Oscillator

The equation for the fundamental frequency of the negative resistance oscillator is:

$$f = \frac{1}{2\pi\sqrt{LC}} \quad (\text{Equation 1.5}).$$

The ability to dynamically change the properties of the components makes the design of the VCO simple. The inductor and the capacitor are the two components that affect the frequency of the VCO. Due to the difficulty of changing the inductance of an inductor, most VCO designs involve changing the capacitance of a capacitor.

There are many experimental techniques being used to electromechanically change the capacitance. Other devices such as diodes and transistors can change the capacitance of the

circuit. There are piezoelectric devices that physically move the plates to create different capacitances. One of the more successful capacitors is by Aleksander Dec and Ken Suyama [5].

The capacitors consist of two parallel plates as shown conceptually in figure 17. The bottom plate is fixed to the substrate. The top plate is anchored to the substrate by a set of springs. When a bias voltage is applied an electrostatic force moves the top plate, therefore, making the capacitance of the capacitor change [5].

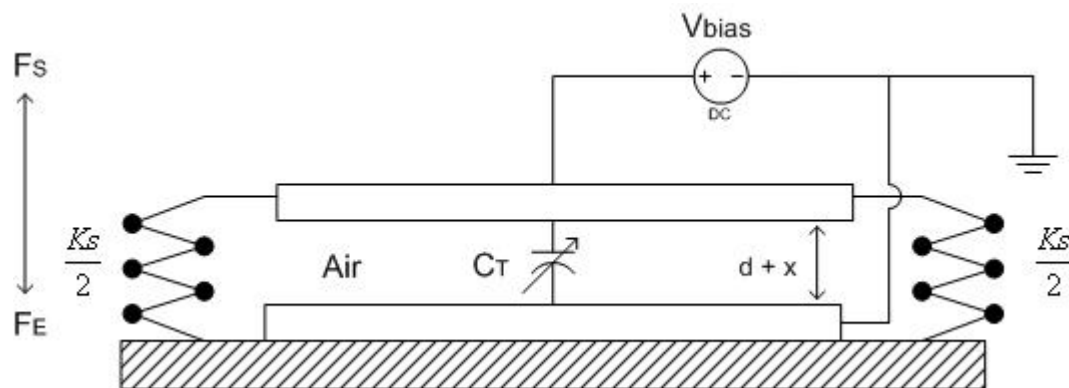


Figure 17. Varactor Capacitor Conceptual

The quality factor of the varactor capacitor is very high, but the capacitor requires a special polysilicon surface micromachining process (MUMP's). The process has three polysilicon layers and a gold layer that is deposited on top of the poly 2 layer as shown in figure 18. The thickness of the gold layer is 0.5 μm . The three poly and gold layers are very expensive to produce.

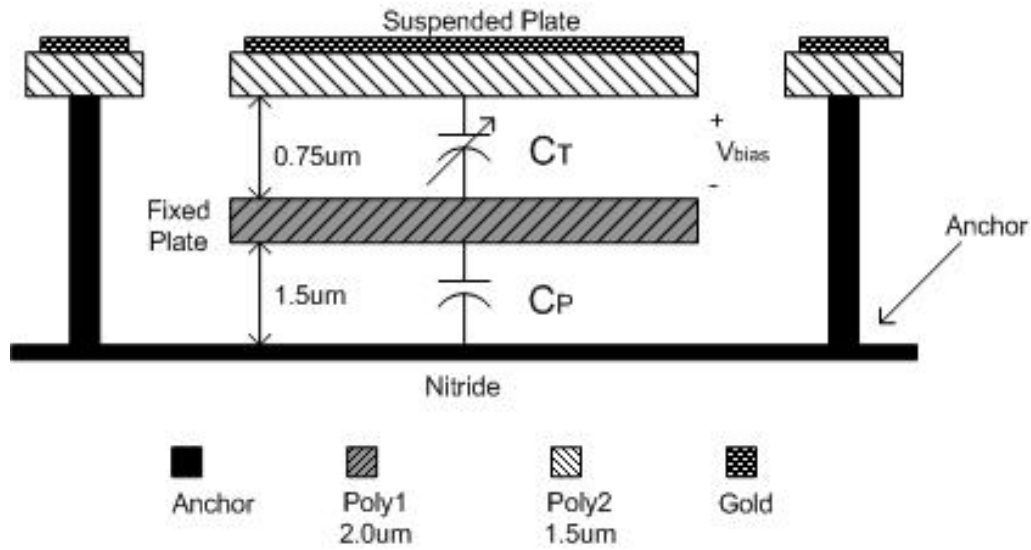


Figure 18. Varactor Capacitor Profile

The advantage of the expensive MUMP's process is the low phase noise that it yields. It also produces extremely high Q values. For special, demanding applications where a high performing VCO is required the MUMP's process may be a suitable selection. A topology that incorporates the varactor capacitors is given in figure 19.

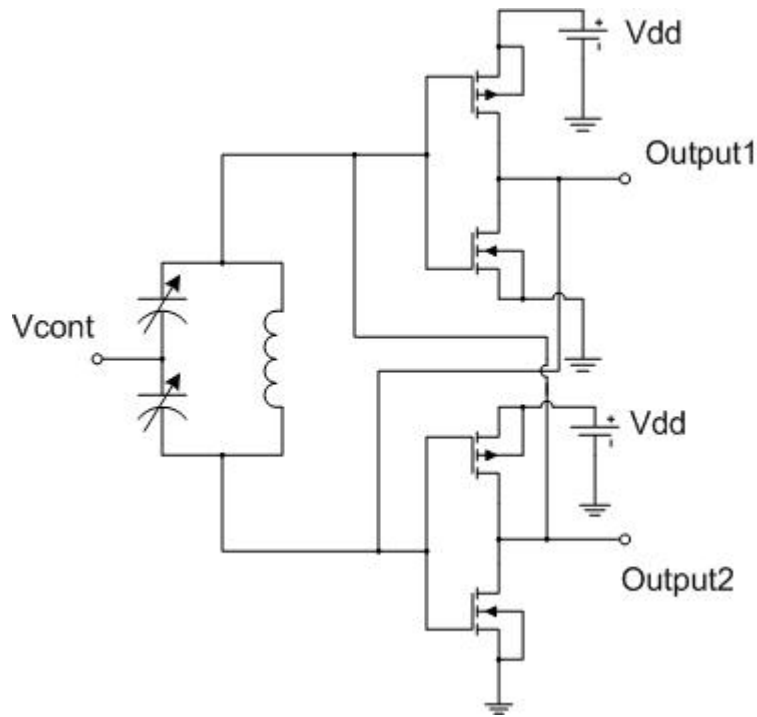


Figure 19. VCO Containing Varactor Capacitors

4.2.3.2 Tunable Diode

A tunable diode is most widely used to electrically alter properties of an oscillator. The varactor diode realizes the voltage-variable capacitance [32]. The LC tank is formed by a regular inductor and the varactor diode. When the control voltage is altered on the anode, the amount of capacitance between the anode and cathode is also altered. A topology of a VCO containing a varactor diode is given in figure 20.

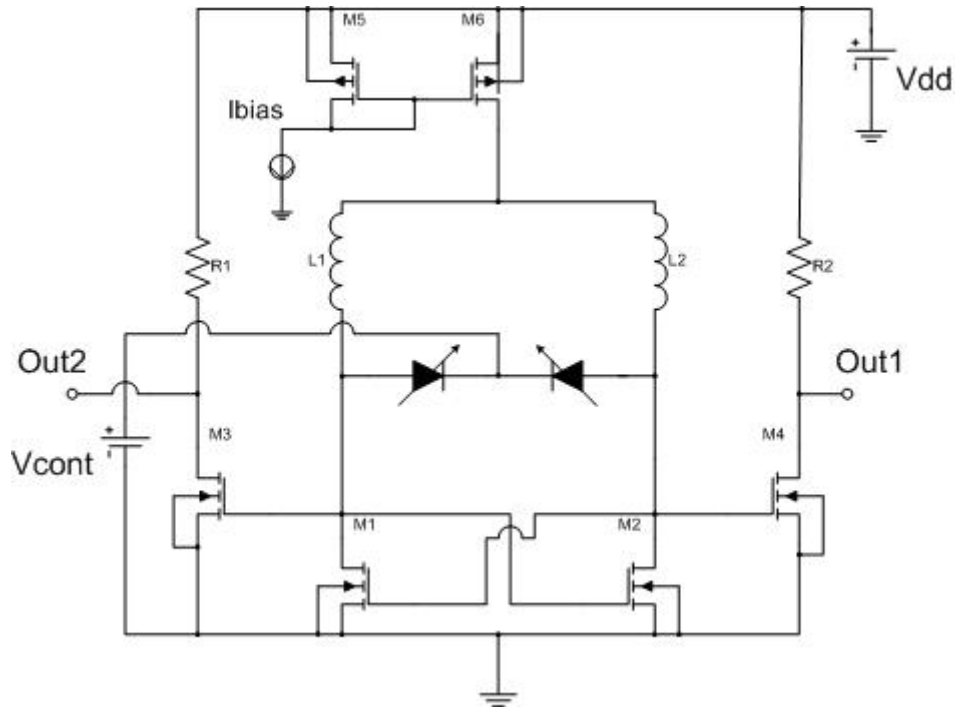


Figure 20. Topology of VCO with a Tunable Diode

4.2.3.3 Varactor Transistors

Another way to dynamically alter the capacitance of a circuit is to use varactor transistors. When the drain, source, and bulk silicon are connected they realize a MOS capacitor. These transistors' performance exceeds that of a VCO tuned by a reverse bias diode varactor.

The PMOS transistors (M5 and M6) replace the capacitors in figure 21. The two PMOS transistors with their drain and source tied to ground form the capacitor. The circuit still behaves like a normal LC circuit, but it has the advantage of not having a capacitor. The PMOS transistors take up less real-estate than the capacitor and produce wider tuning ranges.

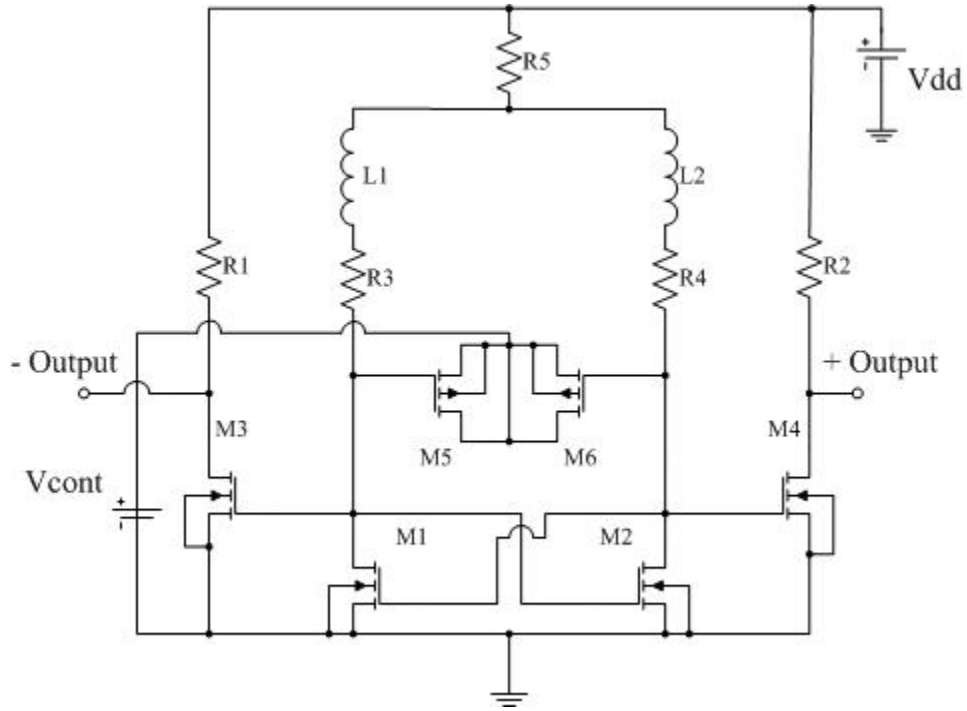


Figure 21. VCO with PMOS Capacitors

C_{ox} is the capacitance between gate and the substrate per unit surface of a PMOS structure. The value of the C_{ox} is determined by the voltage between V_{BG} (Bulk and the Gate) [28]. The capacitance at the transistor gate is varied by changing the voltage applied to the transistor's bulk as shown in figure 22.

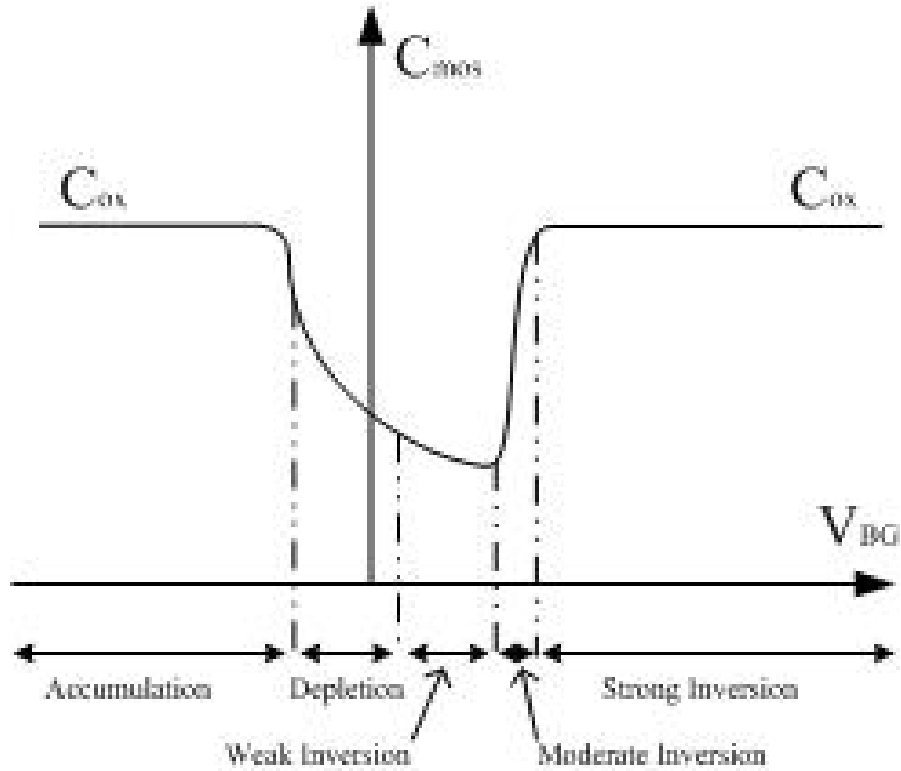


Figure 22. Varactor Transistor with $B = D = S$

Another way to realize a varactor transistor is to limit the transistor to only operate in the accumulation and depletion modes. This type of transistor is known as an A-MOS transistor. Preventing the transistor from entering the weak, moderate, and strong inversion modes prevents the C_{mos} capacitance from climbing back up to C_{ox} . This is done by preventing any injection of holes in the MOS channel as shown in figure 23. A way to achieve that condition is by removing the p^+ doping from the MOS device. Figure 24 shows the A-MOS transistor compared to normal transistor with the bulk, drain, and source tied together ($B=D=S$).

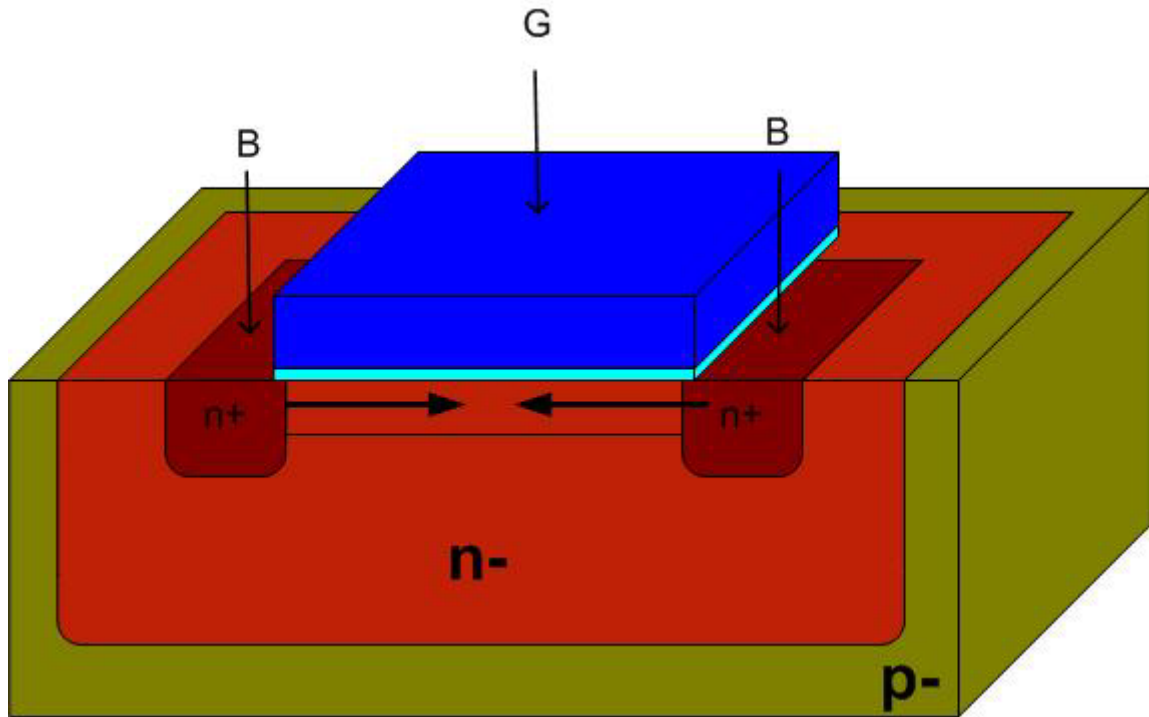


Figure 23. An A-MOS Varactor Transistor Profile

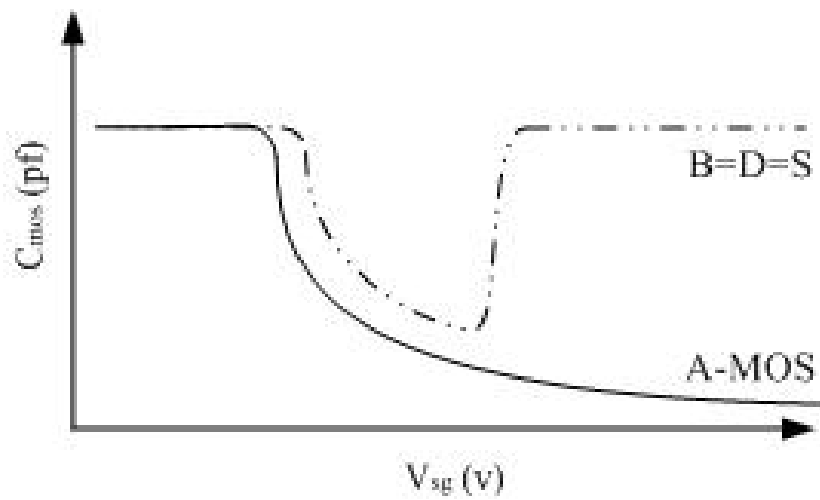


Figure 24. A-MOS vs. B=D=S

The A-MOS transistor outperforms the more popular varactor diode and the traditional B=D=S PMOS as a varactor capacitance. The tuning range of the diode and the A-MOS are both around 11% of the average oscillation frequency, but the A-MOS has lower phase noise [29].

There are other research efforts that are taking place in field of varactor components that are not mentioned in this thesis. This has been an overview of some of the more recent findings. The traditional LC circuits are still used more than any other type of VCO. The cost and quality are usually the reasons for their success. Special applications however do sometimes require special VCOs.

5.0 CURRENT VCO USES

5.1 PHASE LOCK LOOPS

VCOs do not have many traditional uses. They are primarily used in phase lock loops. There are many uses for a phase lock loop (PLL) circuit. In communications, it readily produces many frequencies from one reference frequency. They are used in FM and AM radios as demodulators. They are also used in tone detectors, and frequency synthesizers [11]. In industrial control applications they are used to control motor speeds.

A phase lock loop is made up of three major components, the phase detector, the loop filter, amplifier, and a VCO as shown in figure 25. The phase detector compares the phase of an incoming reference signal with the signal from the VCO, and produces some function of the phase difference. The loop filter helps eliminate unwanted noise. The amplifier then makes the signal stronger. The loop filter and amplifier are optional components in a basic PLL. The final stage is the VCO. The VCO produces the frequency that is a function of the control voltage. The quality of the VCO determines the necessity of a loop filter and an amplifier.

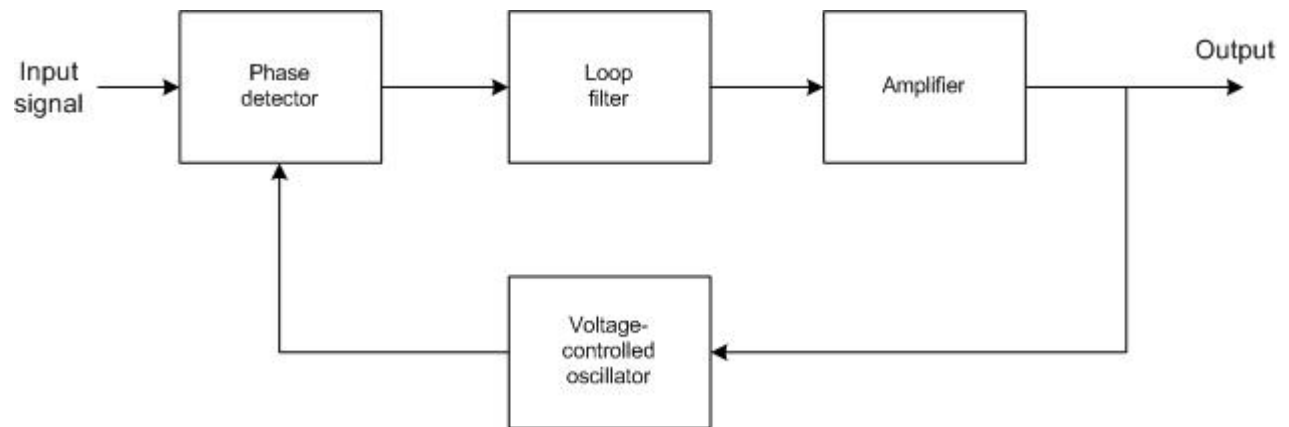


Figure 25. Phase-Locked-Loop Block Diagram

6.0 THE VCO SOLUTION

Testing on-chip antennas introduces a non-traditional use of a VCO. It has historically only been used in phase lock loops, frequency modulation and similar applications. Testing an antenna has never previously been done by using a VCO as a transducer.

For testing an on-chip antenna, a VCO's voltage to frequency relationship is required to be designed, analyzed, and documented. The amount of current the VCO consumes is also documented. The chip with the antennas under test will consist of an energy harvesting antenna, a device that converts the harvested RF energy into DC voltage, a VCO, and a transmitting antenna.

Therefore, when the chip is transmitting an RF signal, the only test equipment that is required is a spectrum analyzer to act as a receiver with a wide band antenna attached to it. The frequency received can be recorded and the previously voltage documented can be generated by using a simple lookup table (Table 2).

The wireless testing of the energy harvesting ability of the antenna also allows the maximum range of the chip transmission to be tested. The test equipment does not need to be attached to the chip.

7.0 ANALOG SUPPORT CIRCUITRY

Support circuitry as shown in figure 26 is required in order for the VCO to test the antenna's efficiency. The harvested energy from the antenna must be converted from RF energy into usable energy, DC voltage, to power the VCO, by a charge pump. The efficiency of the charge pump must be very good in order to accurately measure the quality of the antenna. If a high quality charge pump can not be obtained, then its losses must be predictable.

A matching network between the charge pump and the VCO is necessary for maximum power transfer. The size of the load of the VCO will also determine the amount of power transferred. The size of the load and the maximum amount of power transferred are directly proportional. Another matching network is not necessary, but helpful between the VCO and the Amplifier.

The amplifier boosts the signal from the VCO making the relatively faint signal from the VCO large enough to be picked up over any ambient RF noise present in the testing environment. The amplifier must be a wide band to cover the tuning range of the VCO. The center frequency of the amplifier should be near the center frequency of the VCO.

The amplifier's output is then sent to the transmitting antenna. The antenna does not need to be perfectly tuned to transmit the VCOs frequency successfully. It must however be tuned well enough to transmit a signal that is considerably higher than the noise in the test environment. The quality of the transmission is not vital because only the frequency is needed. The flow of the complete circuit can be seen in figure 26. As long as the communications system, path and channel are linear, the frequency will not change.

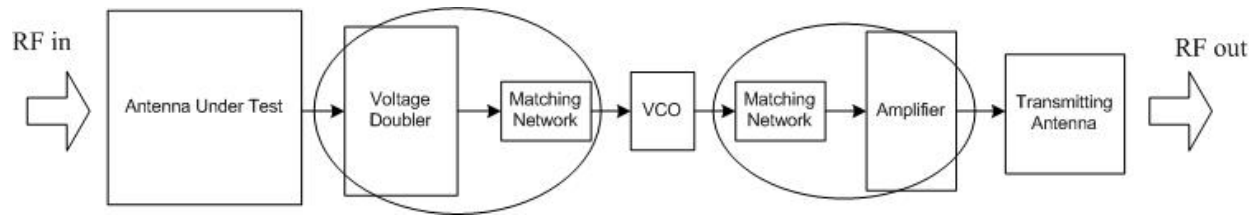


Figure 26. Support Circuitry Flow Chart

7.1 SPIRAL DELTA ANTENNA

The antennas to be tested are spiral delta antennas. The frequency of the antenna is inversely proportional to the size of the antenna. Therefore, there is an advantage to using higher frequency. The disadvantage of using the higher frequencies is that they require a more advanced CMOS technology. The advanced technology typically is more expensive.

The spiral delta antenna in figure 27 is a spiral inductor designed for a specific frequency, 915 MHz, with a resistive impedance at its resonant frequency. The purpose of using 915 MHz is because that is one of the frequencies which are specified for experimentation i.e., the Industrial, Scientific and Medical (ISM) Band. The harvesting antenna's dimensions are 1600um x 1600um in the current technology we are using.

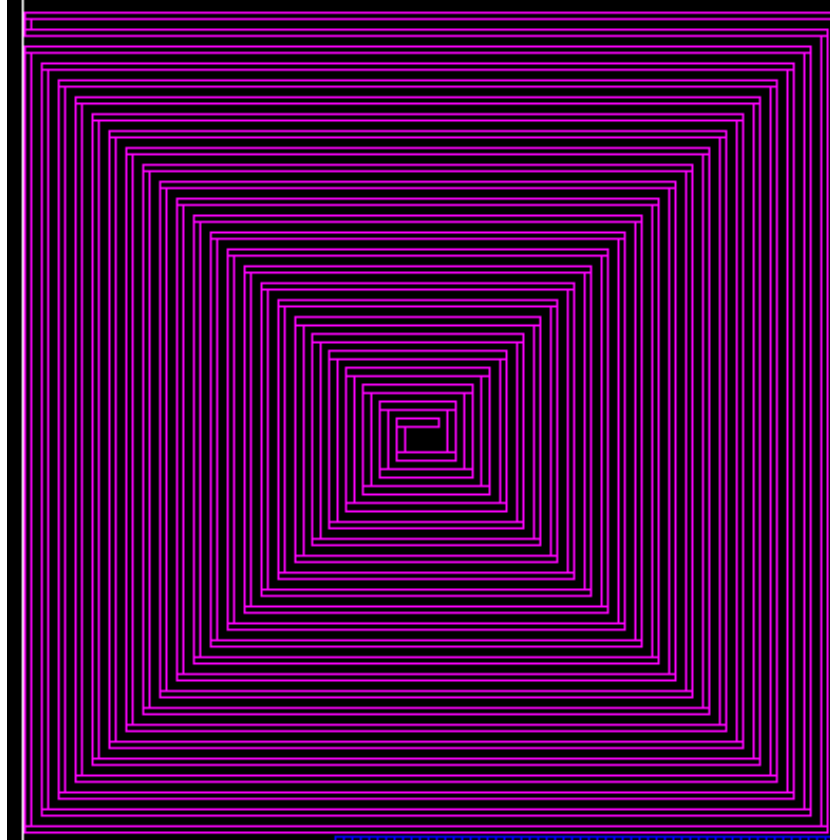


Figure 27. The Spiral Delta Antenna

7.2 CHARGE PUMP

The charge pump, or voltage doubler is a very important aspect in the design. It converts the AC power into useable DC power. In general, power is a constant (in the ideal case), while voltage is increased at the expense of current i.e., constant power. The efficiency of this component will help determine the amount of source power needed to be directed at the chip, and consequently the maximum distance at which the chip will be effective.

A voltage doubler can be implemented with two diodes and two capacitors as shown in figure 28. The layout of the voltage doubler is shown in figure 29.

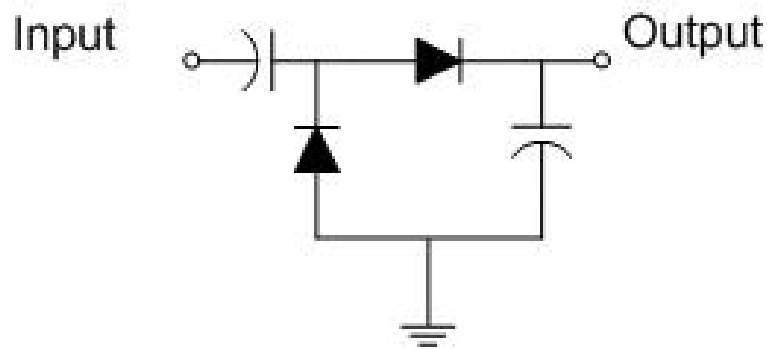


Figure 28. Voltage Doubler

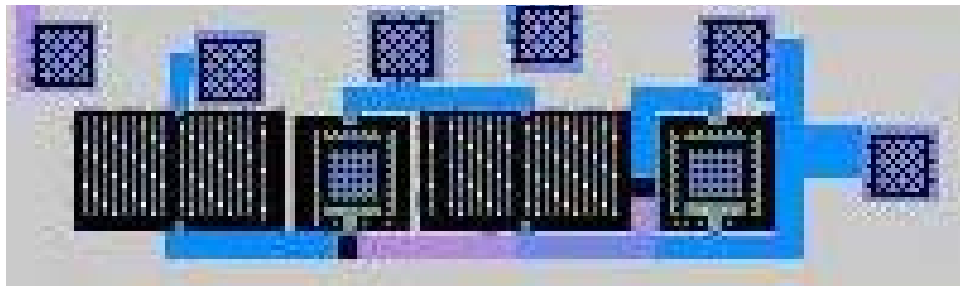


Figure 29. Voltage Doubler Layout

7.3 IMPEDENCE MATCHING

In order to achieve maximum power transfer between devices, impedance matching must be implemented. The matching networks are implemented between the charge pump and the VCO, and between the VCO and the amplifier. A simple π matching network can be used for the matching, where X_1 , X_2 , and X_3 are capacitors or inductors (figure 30).

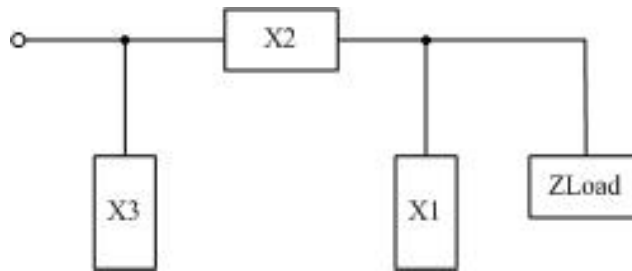


Figure 30. A Simple π Matching Network

An impedance network can be optimized for maximum voltage or for maximum current exchange. A normal matching network is designed to transfer maximum power, of course, resulting in a particular current and voltage. A technique of impedance miss-matching is sometimes used to maximum the voltage of the transfer. This is important because the voltage must be large enough to turn on and off transistors.

7.4 AMPLIFIER

The amplifier is necessary for transmitting the VCOs output frequency with sufficient power to communicate with a receiver. The signal from the VCO is usually not strong enough to transmit a reasonable distance without being amplified. The signal can easily be received in a shielded room, but such a laboratory would not make a reasonable test environment for testing practical antenna efficiencies.

The amplifier used to amplify the VCOs voltage is a typical low noise amplifier with a wide tuning range to cover the range of VCO frequencies.

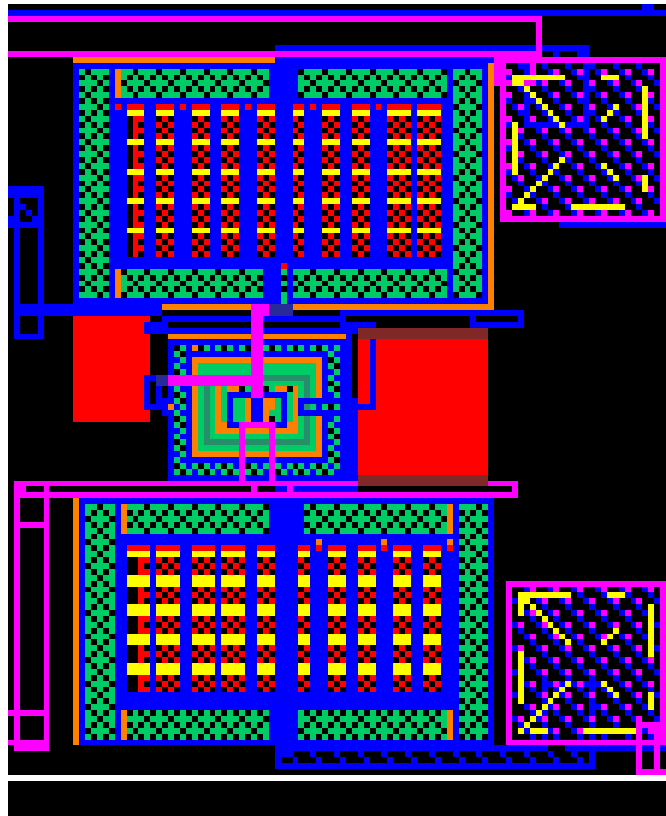


Figure 31. Low Noise Amplifier

8.0 AVAILABLE TECHNOLOGIES

The technology that we used for our fabrication was very outdated and inexpensive. We make use of the AMI ABN 1.5 process. The process consists of 2 polysilicon, 2 metal layers, 1.5 micron, 5 volts operation, n-well, CMOS, technology. The advantage of using the older technology is the inexpensive fabrication price. A 0.5 micron fabrication would have cost us five times as much per run. We primarily were concerned with fabricating analog circuits so the limited metal layers, and high voltage was not as critical. The older technology did however make some designs, and layouts challenging.

Designing a low powered VCO to fit the specific project requirements, discussed later, was difficult with the AMI ABN 1.5. The necessity for multiple prototype runs prevented us from choosing a more expensive technology. The antenna designs that were fabricated with the VCO circuitry did not require an advanced technology to achieve the required results. With the inexpensive technology, the antennas could be tested and redesigned for a fraction of the cost of a more advanced technology.

We did consider moving to a more advanced technology. AMI's C5N was the most favorable among the considered processes. This 0.5 micron technology has 3 metal layers, 2 polysilicon layers, 5 volts operation, n-well, CMOS technology. The C5N technology would have allowed us to decrease the size of the chip. The 5 volts required for operation was the reason that prevented us from moving to it. The size of the digital circuitry, needed for an ID TAG, would be reduced, but the amount of power required to run it would not.

In order to simulate and test the circuit before sending it out for fabrication the detailed technology files are required. Attaining the detailed technology files for some fabrication processes was not possible. The confidential files had been available to educational groups. MOSIS, a low-cost and small-volume prototyping service, changed their policy, and will not release the required files to non-commercial groups [34].

Another reason for not moving to a more expensive technology was the lack of multiple polysilicon layers. The majority of processes only have one polysilicon layer available. The multiple polysilicon layers are important in the design of capacitors. The size of the capacitor would greatly increase if the capacitance was formed with a metal layer. The reduction in size due to the smaller feature size would be forfeited due to the size of the capacitors.

9.0 THE VCO DESIGN AND VERIFICATION EXPERIEMENTS

Two experiments were completed as steps to using a VCO to test energy harvesting antennas. The first experiment was to design, simulate, fabricate and test a low powered VCO.

The second experiment was to transmit the VCOs frequency to a receiving antenna and measure its results on a spectrum analyzer using a connected voltage source. These results were compared with the results from the first experiment and are reported in this thesis.

9.1 OSCILATOR DESIGN

9.1.1 Experiment Description

9.1.1.1 Objective

The objective of this experiment was to design and fabricate a low powered voltage controlled oscillator with a predictable linear frequency range. The function of the VCO is to test the amount of power harvested by an antenna. The phase noise and Q (quality) factor of the circuit were not as important as a constant K_{vco} . A constant K_{vco} would lead to a linear input voltage vs. frequency curve. The advantage of a linear curve is the precision of mapping the input power with the output frequency. A linear curve will allow more accurate conversions for received frequencies between the measured points.

A wide frequency range is also important. A wide frequency range will decrease the amount of error in calculating the input voltage. If the tuning range of a VCO is over 100 MHz then an estimation of a specific frequency on the curve will be close, whereas if the tuning range is 10 MHz then the magnitude of the error can be much greater.

The design was also to be made as small as possible, i.e., minimum area of chip real-estate. The amount of space that is available on future chips may be limited. The VCO is going to be used to test the antennas and should not take up too much of the chip's area. It has also been shown in other research efforts that the circuitry in the area of an antenna will affect the performance of the antenna. Large antenna designs may be necessary and the VCO should not prevent a large antenna from fitting on the chip.

9.1.1.2 Background Information

Topology Selection

There are a number of different topologies that could be used as a template for the VCO. A current-starved ring oscillator was chosen as the topology for the VCO design. The reason for this selection was the current starved topology consumes less power than the other VCO topologies. The majority of documented VCO topologies require more power than tolerable. It also has the widest tuning range and is smallest in chip area used. The tuning range of the current starved oscillator is nearly six times the size of the next best topology. The size of the current starved oscillator is also a fraction of the size of any other topology. The reason for its small size is due to the lack of large components like capacitors, inductors and diodes. The transistors used are extremely small compared to those used in other topologies. Its largest transistor is typically smaller than the smallest transistor used in an LC VCO.

The lenient requirements for the quality of the signal also make the current starved oscillator the topology of choice. The phase noise of the current-starved oscillator is poor compared to most other topologies. The phase noise has very little bearing on our future use of the VCO so this negative factor is not important.

Its other major flaw is the low Q values. The Q value is normally important in most applications. The low Q is acceptable due to the large tuning range of the VCO. The frequency may be shifted slightly in either direction due to the lack of quality of the circuit, but the little shift will be a small percentage of change with respect to the tuning range. Therefore, accurate measurements can still be achieved.

Overall the current starved oscillator fits the requirements the best. It is best suited in the areas of importance and has weaknesses in areas that are not critical. It is also much easier to design than most of the other topologies.

Oscillator Design

There were a multiple current starved oscillator topologies to choose from. The topology that was chosen was the basic current starved oscillator in figure 12. The performance differences between that oscillator, the simple oscillator (figure 13), and the full oscillator (figure 11) are very subtle. The reason for this selection was the buffer on the output that strengthens the signal.

Sizing the components was the next task after choosing a topology. In order to conserve space the smallest transistor sizes possible were used as shown in figure 32. The PMOS transistors in the ring oscillator loop are the minimum size, $4.5\ \mu\text{m}$. The NMOS transistors were sized at $18\ \mu\text{m}$. The larger NMOS transistors are necessary to pull the signal back down to ground.

The current starved transistor, M3, is sized at $60\ \mu\text{m}$. It must be at least 3 times the size of the NMOS transistors in the ring oscillator for it to draw enough current to greatly affect the propagation delay in the ring. The output buffer is simply two inverters. The PMOS is also minimum width and the NMOS is twice the size.

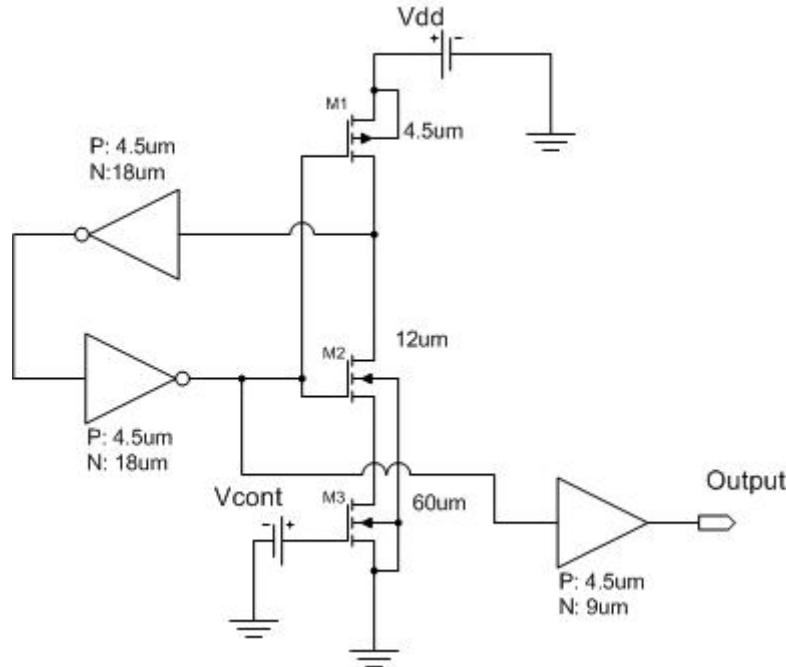


Figure 32. Current Starved Oscillator with Sizes

Simulations

Oscillators are difficult to simulate due to their physical inability to start without any external input signals. Simulators have difficulty during the start of the oscillation due to needing to initiate the circuit noise's effect on the unstable circuit. Oscillators operate in an unstable state and require a little bit of noise or jitter to get jumpstarted. Software normally doesn't account for such noises in a circuit, resulting in making it difficult to initiate oscillation.

There were two software packages available for this research that took into account the necessary circuit noise required for oscillation. The two software packages were Ansoft's Serenade, and APLAC. The two software packages solve these problems differently.

APLAC requires the user to manually input the predicted noise. It accepts a current at a specified frequency. The specified noise is then injected into the circuit at a point that must be specified. Due to unpredictable process variations and complex calculations needed to predict

other circuit noise that may affect the start of the oscillator, a successful simulation of this is very difficult. A brute force method can be applied checking all possible frequency and currents in a certain range. These simulations can be very time consuming, in some cases taking 47 hours to complete. Figure 33 is the current starved oscillator in APLAC.

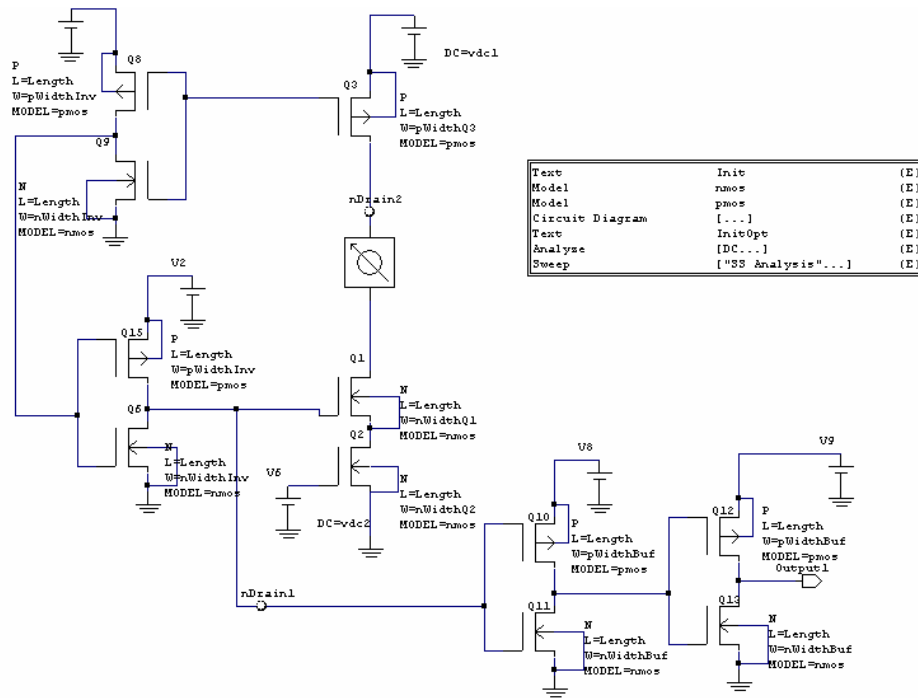


Figure 33. APLAC's Oscillation Simulator

The other software package, Serenade, uses a similar, but simpler approach. This software also injects a current, but looks for a negative current in the feedback loop. A negative current is a sign that the circuit is unstable and will begin to oscillate in a normal environment. The user must specify the injection point, and the software chooses the frequency and current. The simplicity of their scheme and the output information are more useful than that of APLAC. The schematic in Serenade is shown in figure 34.

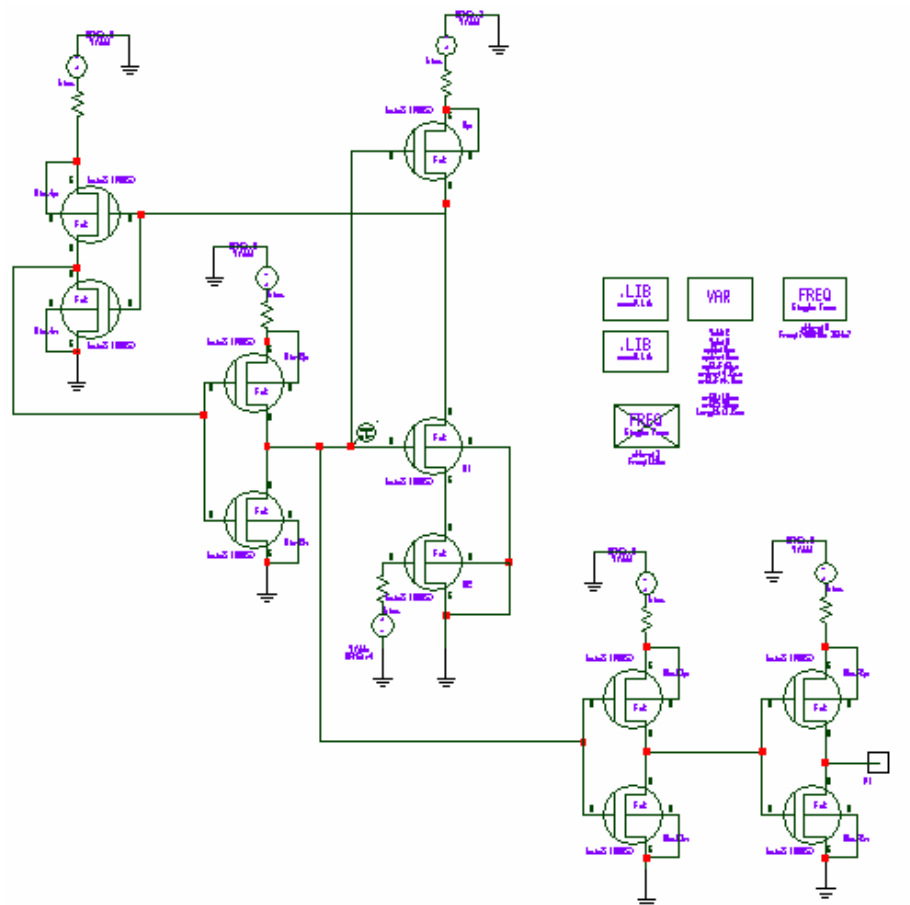


Figure 34. Ansoft's Oscillator Simulator

9.1.1.3 Test Setup

Chip layouts

Four VCO designs that met the predetermined design requirements were successfully fabricated and tested.

One single chip was used in this experiment to fabricate all four designs. The chip contained two patch antennas on the top and the bottom and four VCOs spaced out through the middle. The two patch antennas shown in figure 35 were used in a different experiment and are not a part of the current VCO research.

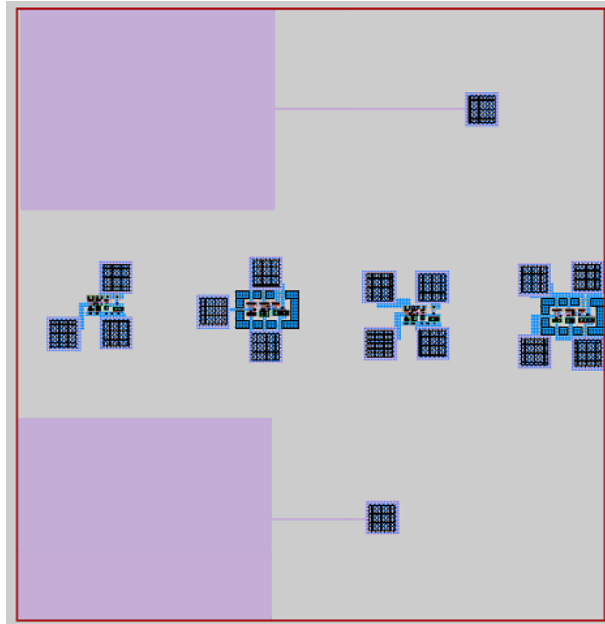


Figure 35. VCO Chip with the Patch Antennas

The current-starved topology has many characteristics similar to a digital circuit. It uses relatively small transistors, and it does not contain any inductors, resistors or capacitors. Those characteristics make it difficult to use normal analog layout techniques. Normal analog layout techniques would include mirroring, dummy elements, using unit sizes, separate guard rings, and fingered transistors to name a few. Due to the lack of strictly analog qualities the same circuit was designed in both an analog and a digital style layout.

A differential analog circuit will have two of each component. The mirroring layout technique makes two identical layouts of the matching component and then positions them so the component is symmetrical. An example of a symmetrical circuit can be view in figure 36.

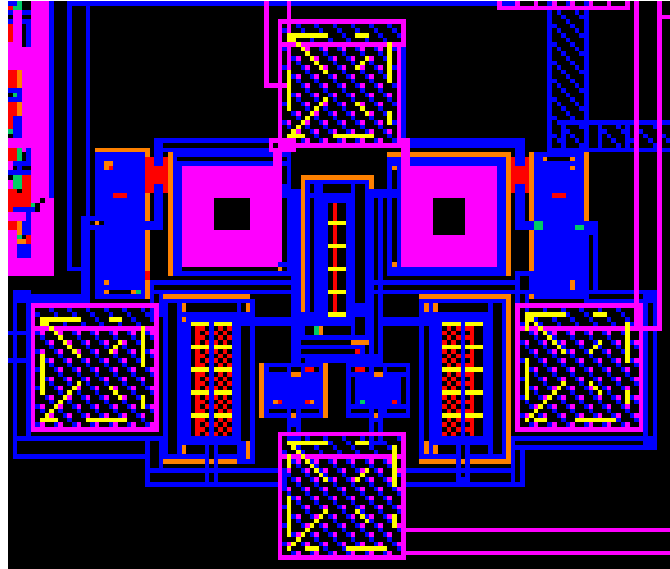


Figure 36. Example of a Circuit Using a Mirroring Technique

Dummy elements are used to protect metal layers from inconsistent process itching. The dummy elements are placed on the outside of the element that it is to protect. This prevents the inner elements from receiving less itching than the outer elements during the fabrication process. A block diagram using dummy elements is in figure 37.

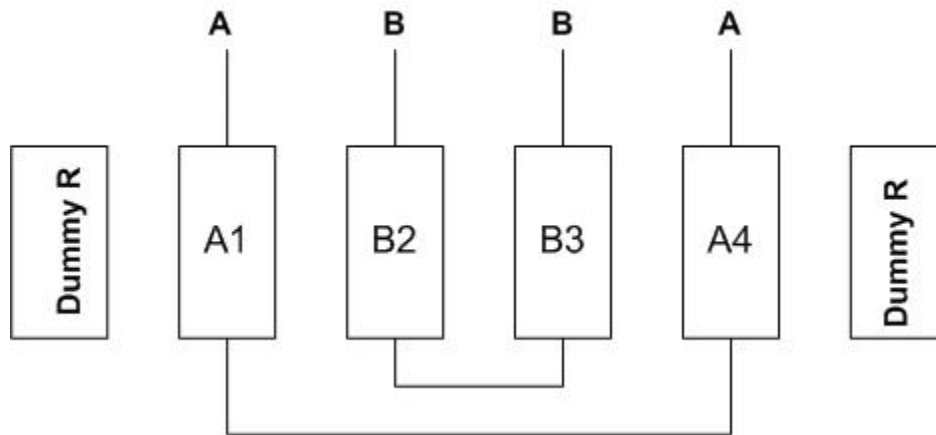


Figure 37. Dummy elements outside of the protected elements

Unit sizes are important to keep the ratio of process etching effects consistent from component to component of different sizes. Only the outer edge of a component is affected by etching. A unit can be made with different dimensions resulting in a different amount of edge that is exposed to etching effects. Using unit sizes will allow two elements of different sizes receive the same percentage of etching effects. In figure 40 three different capacitors are using basic unit blocks to form the specified size. The center capacitor is one unit block. The middle two on the top and bottom are two unit blocks and the third is formed by the four unit blocks in the corner. Figure 38 is an example of using an unit to make larger components.

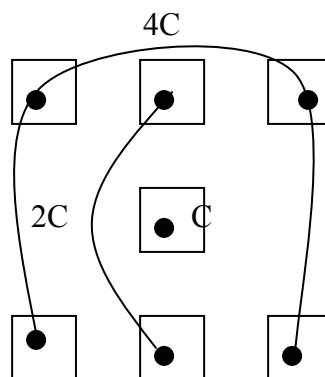


Figure 38. An example of using unit sizes

Guard rings are metal layers that are tied to the substrate. They are used to shield unwanted noise from entering your circuit. Analog circuits use separate guard rings around each element of a circuit. A digital circuit does not have separate guard rings due to the signals not needing to be protected. A large guard ring protects the chip from other elements on the same board. That guard ring is incorporated in the pad frame. An example of a guard ring is indicated by the arrows in figure 39.

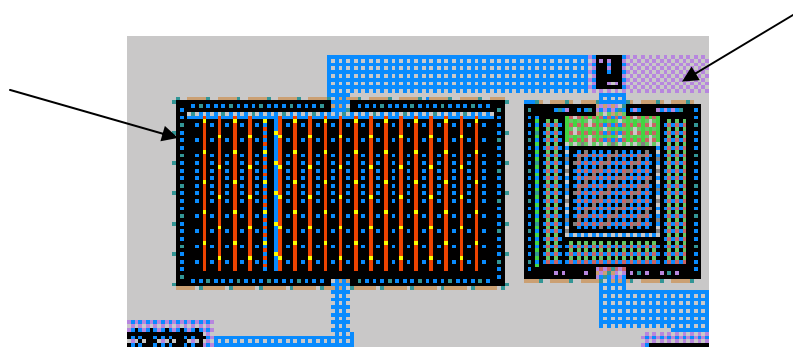


Figure 39. An example of a guard ring

Fingering is a technique that is used when designing capacitors. The capacitor pads are divided into equal limbs or fingers. These fingers add up to total the desired capacitance. The resistance is in parallel due to the multiple fingers resulting in less parasitics in the circuit. Figure 40 shows an example of a capacitor using the finger technique.

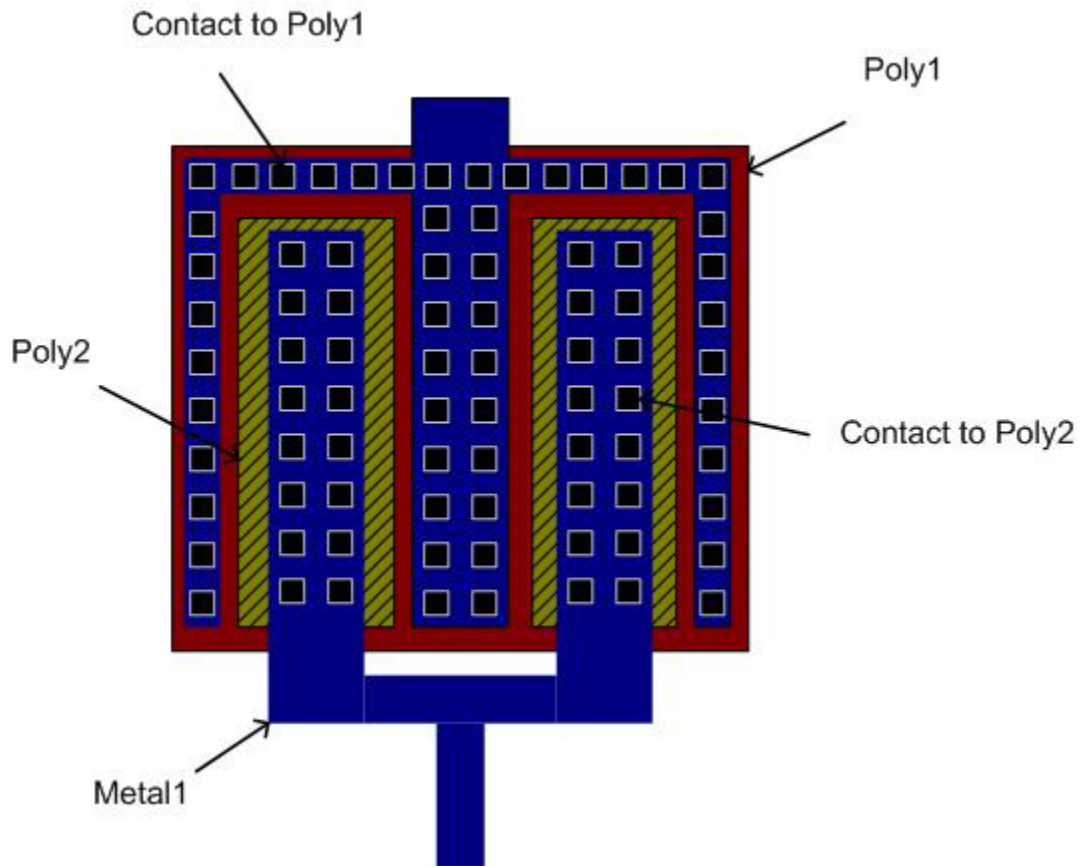


Figure 40. An example of a capacitor using the finger technique

The first VCO tested and discussed here is the digital style layout. This design includes traditional digital layout techniques. The power and ground rails are long metal traces that gives all of the transistors in the area easy access to either GND or VDD. The PMOS transistors were all connected by one power rail. The NMOS transistors were all tied to one ground rail. The transistors for the most part were not made with fingers. A common tub mask was used for all of the PMOS transistors as shown in figure 41.

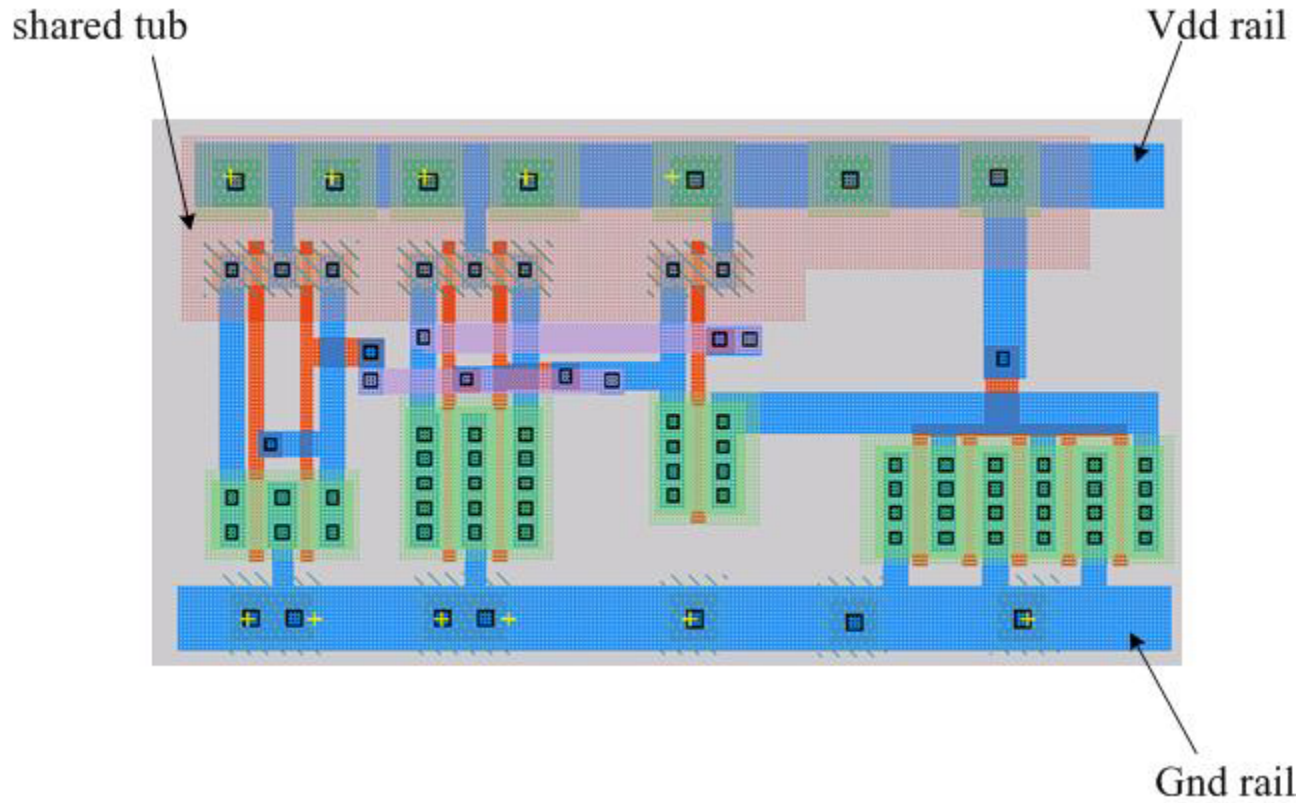


Figure 41. Digital Style VCO layout (VCO1)

The second VCO was an analog style layout. The transistors do not share a common rail for ground or power. The transistors were designed with fingers. Each PMOS transistor has its own tub mask layer. There is a ground ring which encloses the entire circuit as shown in figure 42.

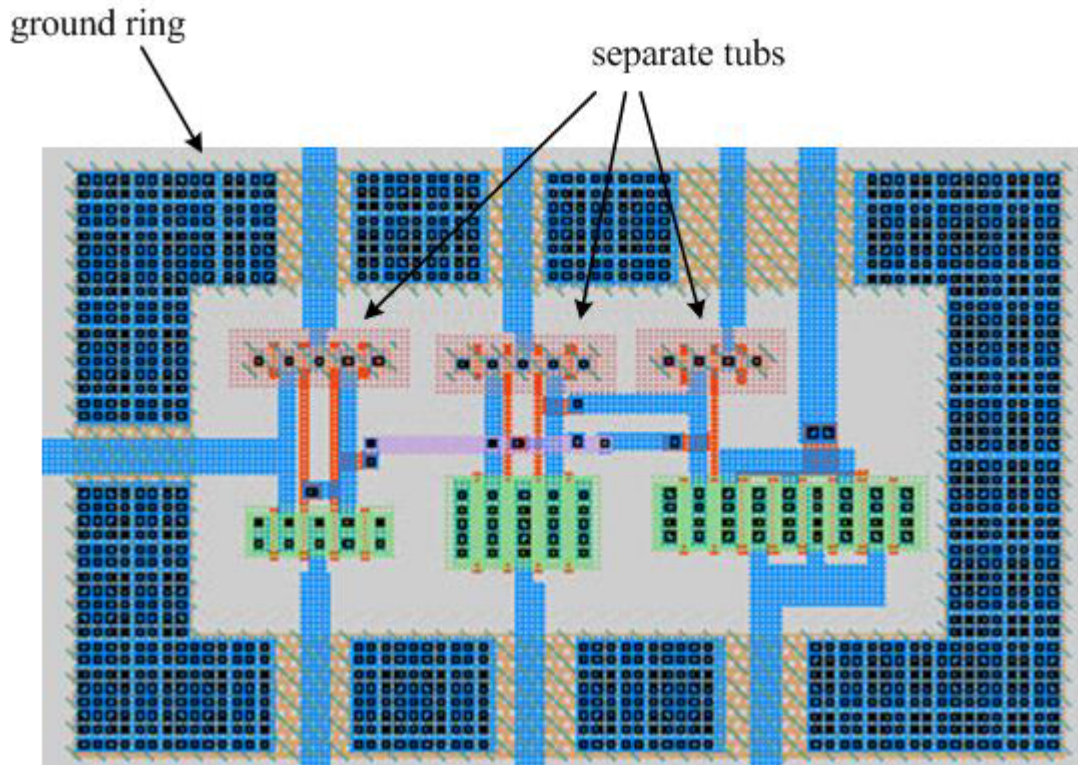


Figure 42. Analog Style VCO layout (VCO2)

The first two VCOs had the VDD and Vcont inputs wired to the same pad. The third and fourth VCOs were made exactly like the first and second respectively, but the VDD and Vcont inputs were wired to different pads instead of sharing one common rail. The reason for that is so the noise from one power source does not affect transistors attached to the other power source.

The advantage of connecting the VDD and Vcont inputs is only one power source is required. Only needing one power supply allows the VCO to be directly connected to the antenna in future experiments. The frequency range is also much wider when they are connected. A disadvantage of connecting the two inputs is the output power is lower when lower voltages are applied to the input. This may affect future testing of antennas that may harvest low voltages. The faint output signal may be difficult to detect.

Test rig

The VCO was put on a test rig so input and output cables can be attached to them. The test rig was made with FR4 printed circuit board (PCB) with copper traces. The test rig has five copper posts and four SMA connectors soldered to it. The posts are necessary to wire-bonding to them. The input/output of the SMA connectors were connected to each of the copper posts. The other copper post was grounded. The VCO test rig can be seen in figure 43.

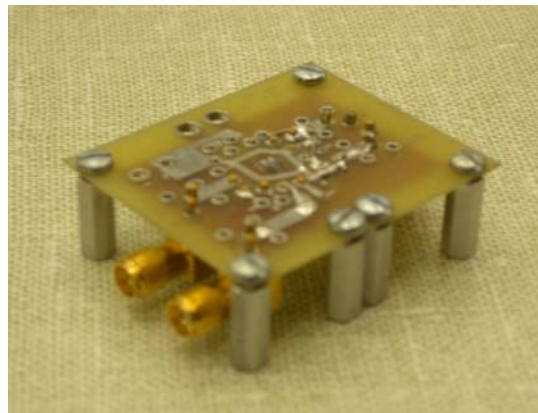


Figure 43. The VCO Test Rig

Wire bonds

To attach the SMA connector the chip containing the VCO wire bonds are necessary. The bonding wire is made of aluminum. Its thickness is $25.4\mu\text{m}$. There are three bonds. The first bond is connected from the ground pin of the test rig to the ground pad of the VCO. The second bond is connected to the pin, which is connected to the SMA input. The third bond was connected from the output pad of the VCO to the input pad of the spectrum analyzer. The three wire bonds can be viewed in figure 44.

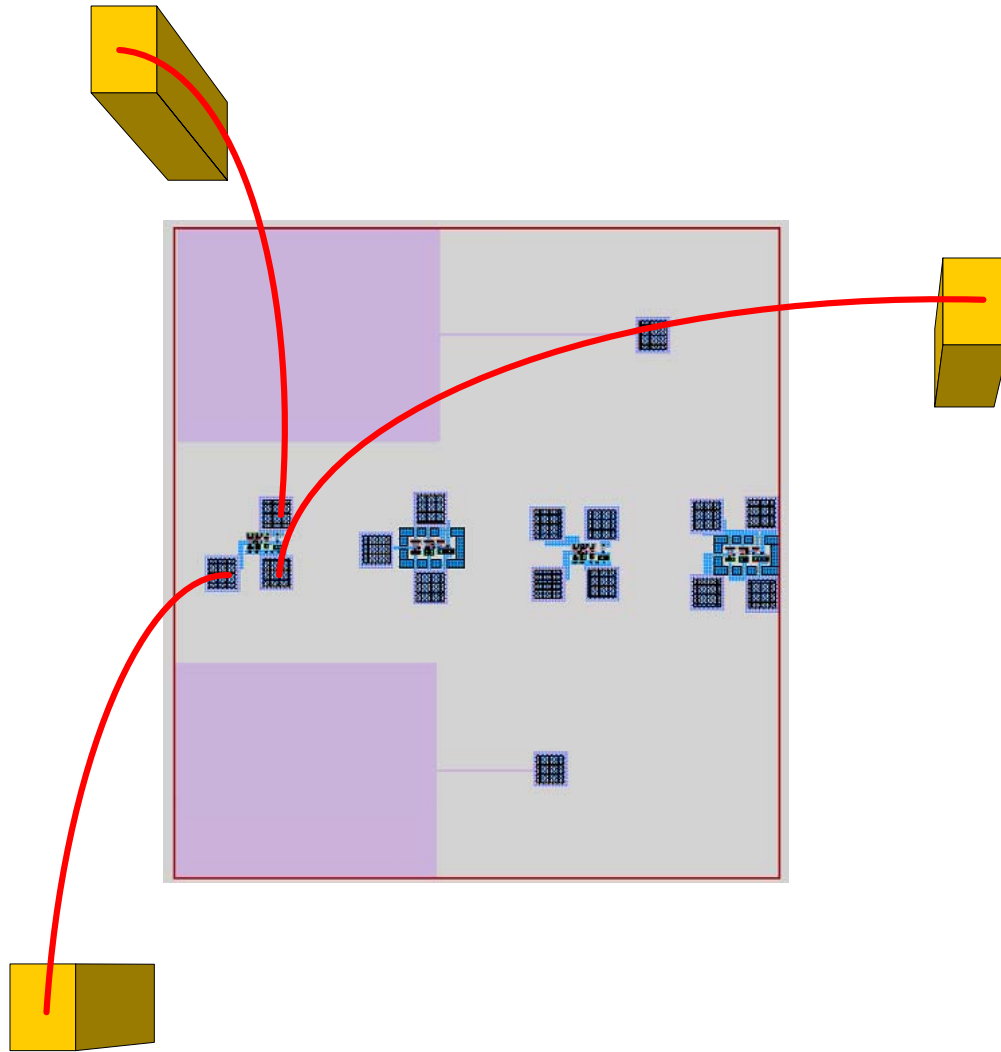


Figure 44. Theta Wire Bonds

Power sources

A simple digital power source was connected to the test rig using SMA connectors with a Pomona 3073 adaptor (figure 45). The power source ranged from zero to six volts (figure 46).



Figure 45. Pomona 3073 Power Adaptor



Figure 46. Power Supply

Network analyzer

An E4403B Agilent spectrum analyzer was used to detect the output frequency. The analyzer was set at a frequency range of 100 MHz to 600 MHz. The range of the test window was 500 MHz. The results can be easily seen in a RF shielded room. The results in an uncontrolled environment had to be averaged to easily observe transmission results.

Equipment Setup

The test required one power supply, a spectrum analyzer, wires for connections and the test rig as mentioned before. The DC power supply was directly connected to the test rig with coaxial cables. The output of the VCO was directly connected to the spectrum analyzer. A diagram of the setup can be seen in figure 47.

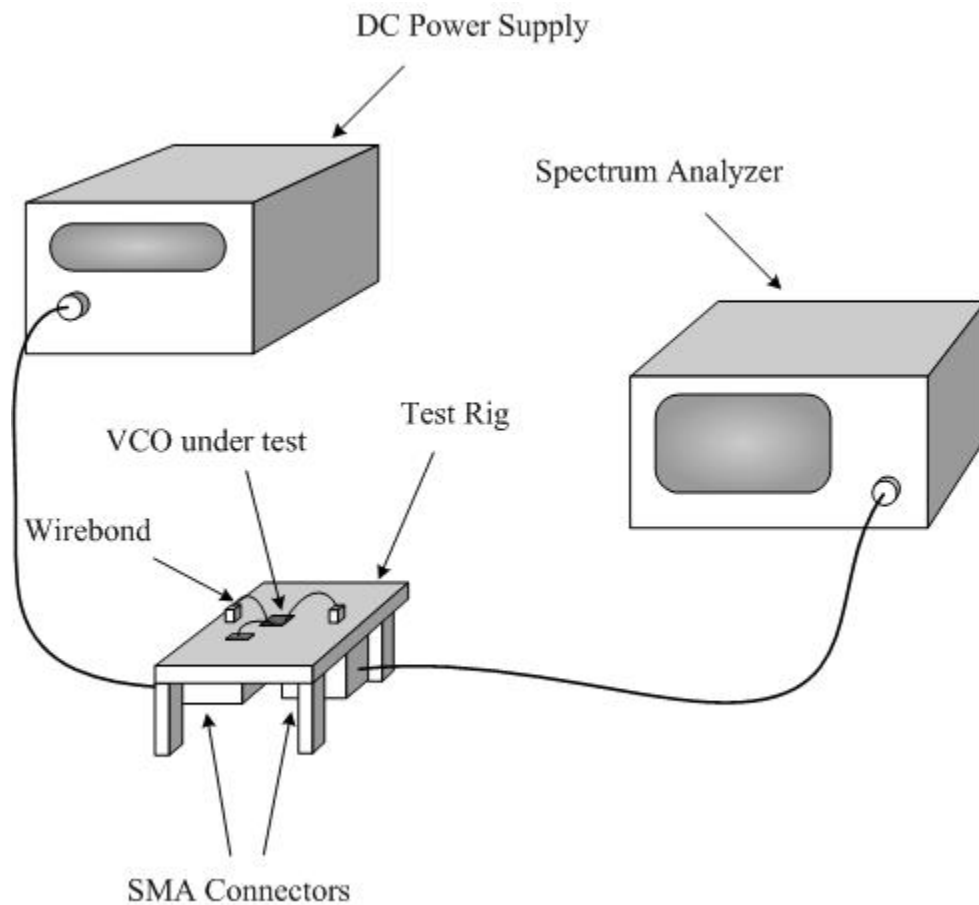


Figure 47. VCO Test Setup

9.1.2 Results

The experiment was a success. All four of the VCOs that were fabricated preformed better than the simulations indicated. The tuning frequency range was about 4 times as wide as the

simulations. The amount of power consumed by the actual VCO (3mW) was also less than the power consumed in simulation (12mW). K_{vco} of the actual layout was closer to constant than expected.

The excellent results are hard to explain for certain. Both simulators use estimations and approximations to determine the output. There is a degree of error in both programs. That may account for some of the difference in the results. The models of the MOS transistors may not have been exactly the same as what was fabricated. The models used were results from previous fabrication runs. There are three chip runs between the results used for simulation and the fabrication. There may have been changes made. The output signal was much weaker than that of the simulation. That explains why less power was consumed. The 1.5 AMI process has a transistor speed limitation. The frequency is in the range, but some gain is lost at that frequency.

Both programs have been known to bad results before. Using their software it is possible to successfully simulate frequencies which are well above the technology's limitations.

9.1.2.1 VCO 1 Results

The first VCO was the digital style layout. The average K_{vco} was 109.06 rads/s/V. The standard deviation was 11.73 rads/s/V. The signal to noise ratio ranged from 2.9 dBm at 1.5v to 30.4 dBm at 6v. Table 2 displays the measured results from VCO1.

Table 2. VCO1 (digital) Analyzer Results

VCO1 (digital)

<u>Voltage</u>	<u>Frequency</u>	<u>dbm</u>
1.5	33.0	-58.9
2.0	86.8	-51.2
2.5	147.7	-47.8
3.0	209.1	-42.7
3.5	268.9	-41.7
4.0	326.0	-38.3
4.5	380.2	-36.5
5.0	431.2	-35.3
5.5	478.9	-31.7
6.0	523.8	-30.7
noise level:		-61.4 dbm
frequency swing:		490.75 MHz

The second VCO, the analog style layout, performed equally as well. The frequency range was less than that of VCO1 by 53.05 MHz. The average KVCO was 97.04 rads/s/V. Its standard deviation was 10.34rads/s/V which was better than the digital VCO. The noise level, -61.94 dBm, was lower than the first VCO. The measured results from VCO2 can be viewed in table 3.

Table 3. VCO2 (analog) Analyzer Results

VCO2 (analog)

<u>Voltage</u>	<u>Frequency</u>	<u>dbm</u>
1.5	41.7	-55.9
2.0	91.7	-47.5
2.5	146.0	-45.5
3.0	200.4	-39.1
3.5	253.0	-37.5
4.0	303.1	-34.4
4.5	351.2	-31.0
5.0	395.6	-30.8
5.5	438.7	-30.5
6.0	478.4	-27.6

noise level: -61.9 dbm

frequency swing: 436.70 MHz

The results of the two the frequency versus voltage are plotted on a graph in figure 48. The two VCOs signal strengths are compared in figure 49.

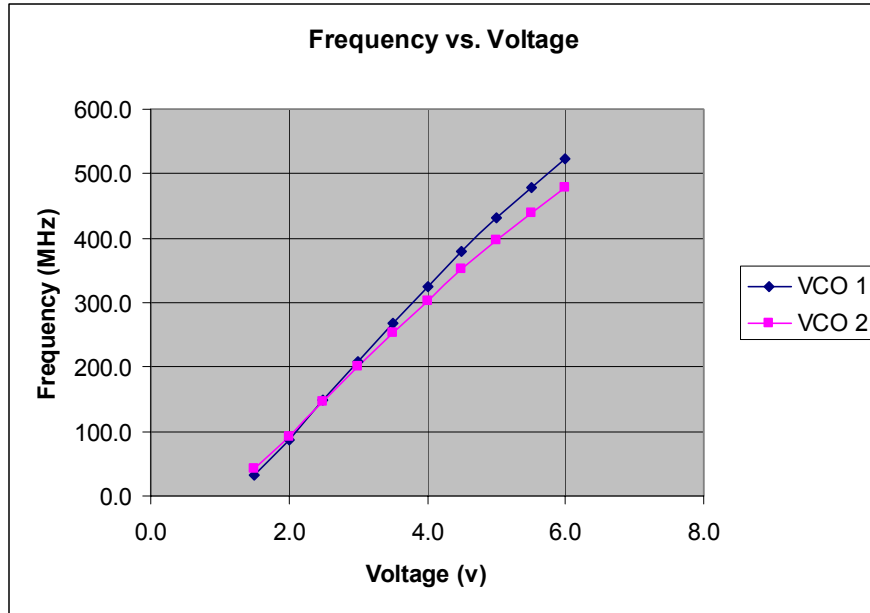


Figure 48. VCO1 and VCO2 Frequency vs. Voltage

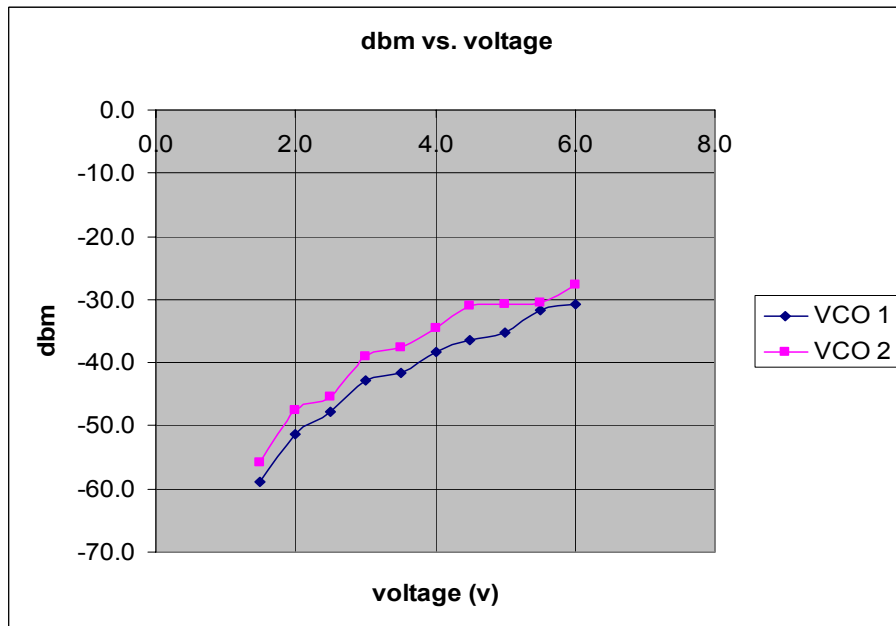


Figure 49. VCO1 and VCO2 dBm vs. Voltage

9.2 TRANSMISSION I EXPERIMENT

The purpose of the transmission experiment was prove the antennas could transmit a VCOs signal and be received. The reason for this step is to prove the antennas transmitting capabilities. The experiment was implemented by simulating the harvesting antenna with a DC power supply and then transmitting the results via transmitting antenna to a nearby receiving antenna which was connected to a network analyzer.

9.2.1 Description

9.2.1.1 Objective

The objective of the experiment was to accurately measure the amount of power being transmitted without touching the chip with test equipment from a connected power source. The results were then compared to the results from the previous experiment. This is intended to prove the antenna's transmitting ability and show consistent voltage verse frequency of the VCO from test to test.

The test will determine if using an amplifier to boost the signal from the VCO could be avoided. The power consumed by the amplifier could make testing the envelope of the antenna's performance difficult. Another reason was to determine what the lowest voltage that could be converted, transmitted, and received in a normal test environment.

The possibility of the faint signal from a non-amplified VCO may not be distinguishable in a normal RF environment. This concern also prompted this test. If the signal to noise ratio is high enough then future tests will not need to be conducted in an RF shielded room. The advantage of

not using an RF shielded environment enables us to test the antennas in some of the actual environments that they might be used.

9.2.1.2 What was accomplished

The experiment successfully transmitted an RF signal from a voltage controlled oscillator, which was used to determine the energy supplied by the power source. It proves the transmitting ability of the delta spiral antenna. This also makes it possible to test the amount of power received from an energy harvesting antenna without connecting test equipment to it. The VCO and transmitting antenna have successfully transmitted the power, therefore when powered by the harvesting antenna and then converted to DC via the voltage doubler the amount of energy harvested can be determined.

The test was conducted in both an RF shielded room and in two different open environments. The first test, in the shielded, room was done to prove that the concept worked. The signal is easier to find on a Spectrum Analyzer due to the interfering noise that is shielded by the room.

The second test was conducted in the laboratory in 570 Benedum Hall. The laboratory test proved that the concept would work in most environments. Other RF devices and testing equipment are also in the room. The signal was strong enough to be distinguished over the ambient noise in the room. Finding the signal was more challenging in that environment, but possible since the outputted frequency is known. If the frequency is not known it can still be found, but may require more time.

The third test was setup in a hotel lobby during as normal business day. The test was setup as a demonstration to show the ability to transmit in a normal everyday environment. It was also a successful. No measurements were taken from this test as the test was demonstrated for various Pittsburgh Digital Greenhouse members.

9.2.1.3 Test Rig Setup

Chip layouts

Two chips were used in this experiment. The first chip, Theta (figure 50), contained two patch antennas, one on the top and one on the bottom and four VCOs spaced throughout the middle. The second chip, Epsilon (figure 51, contains four spiral (delta) antennas, four voltage doublers, and two dipole antennas.

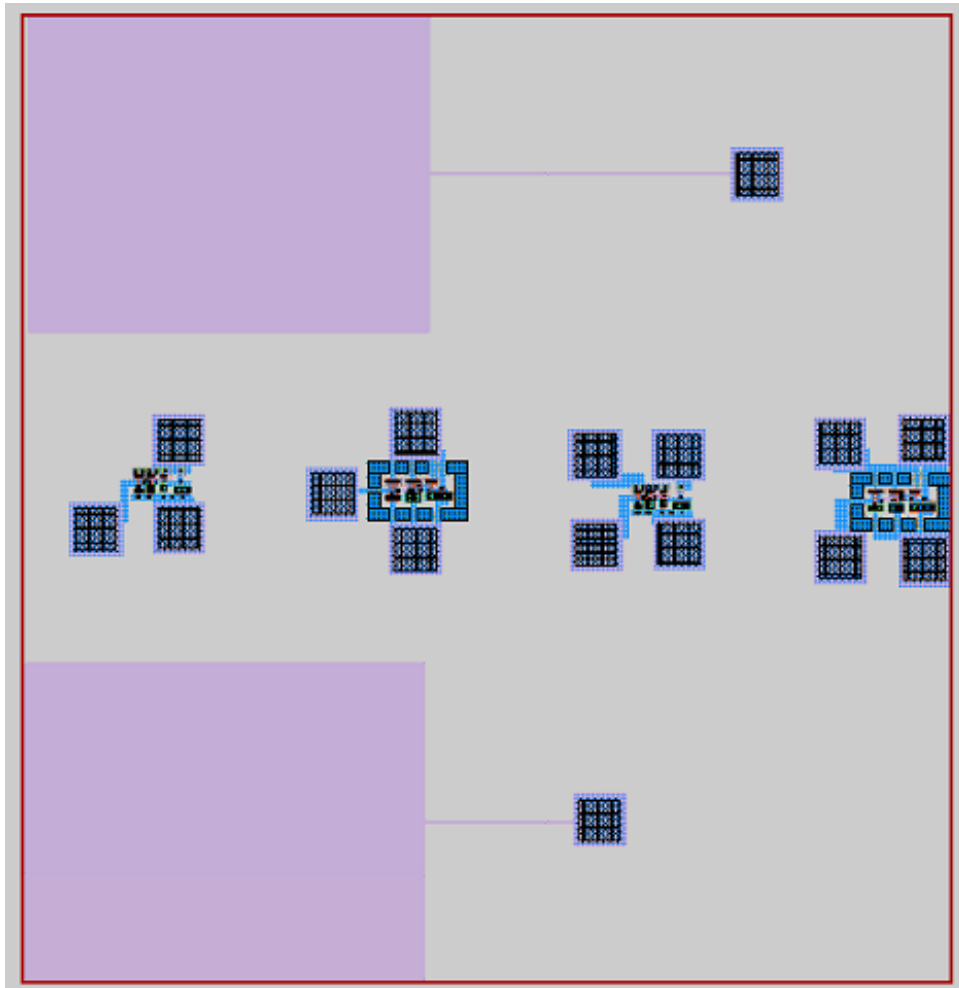


Figure 50. Theta chip

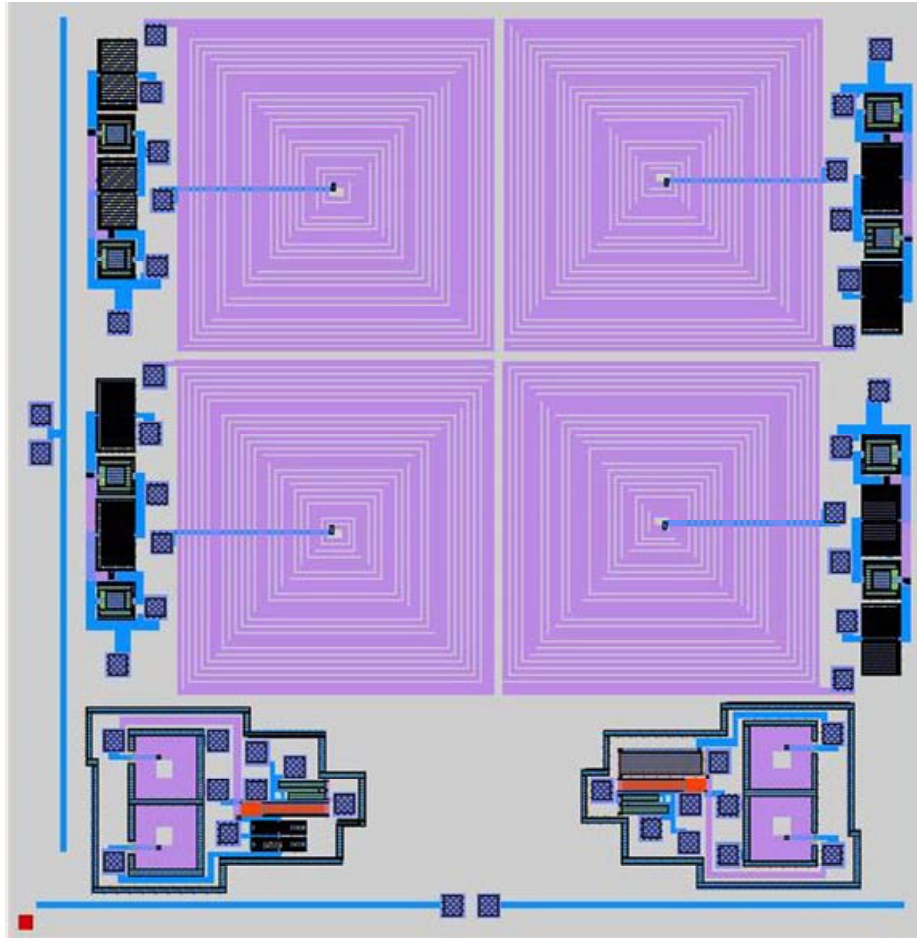


Figure 51. Epsilon Chip

The test only used two components, one from each chip. One of the delta, spiral antennas was used on the Epsilon chip. Only one VCO was connected at any given time from the Theta chip. None of the remaining components on either chip were interconnected. The remaining three delta antennas, the four voltage doublers and the two dipole antennas on the Epsilon chip were not used in the test. They were used in another unrelated test. The other remaining three VCOs and the two patch antennas on the Theta chip were also not used during this test.

Test rig

The test rig is made of FR4 PCB with copper traces. The test rig has two copper posts which were used as pins and one SMA connector soldered to it. The input of the SMA connector was connected to one of the copper post. The other copper post was grounded. A top view of the test rig is shown in figure 52.

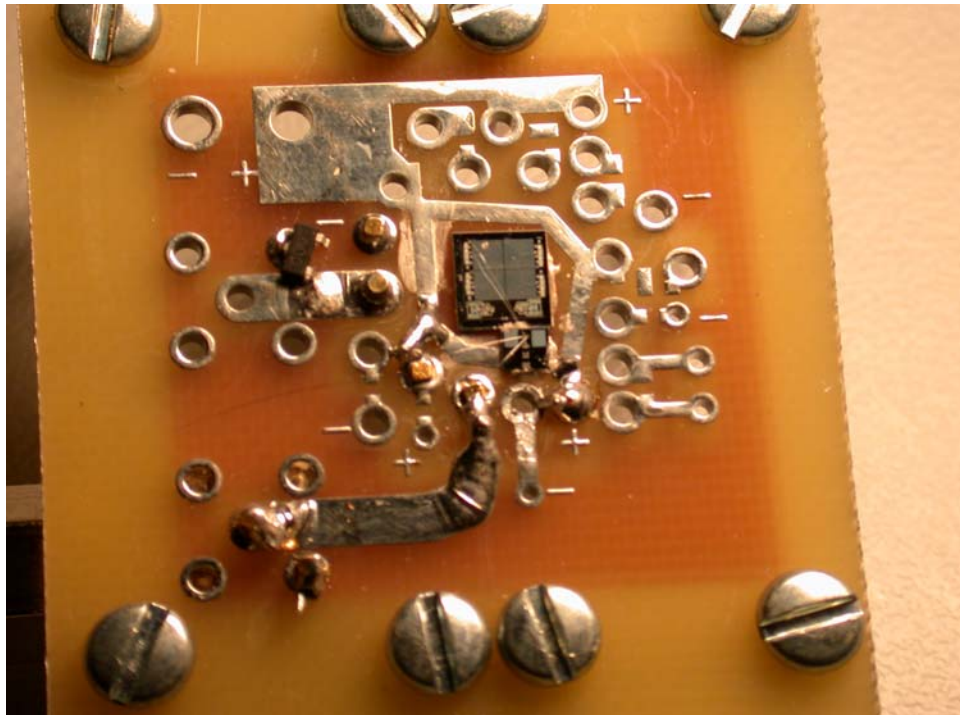


Figure 52. Test Rig

Wire bonds

The bonding wire for this experiment was aluminum wire with a thickness of $25.4\mu\text{m}$. There were three bonds. The first bond was connected from the ground pin of the test rig to the ground pad of the VCO. The second bond was connected from the VDD, SMA input to the input pad of the VCO. The third bond was connected from the output pad of the VCO to the input pad of the antenna. The bonds can be seen in figure 53.

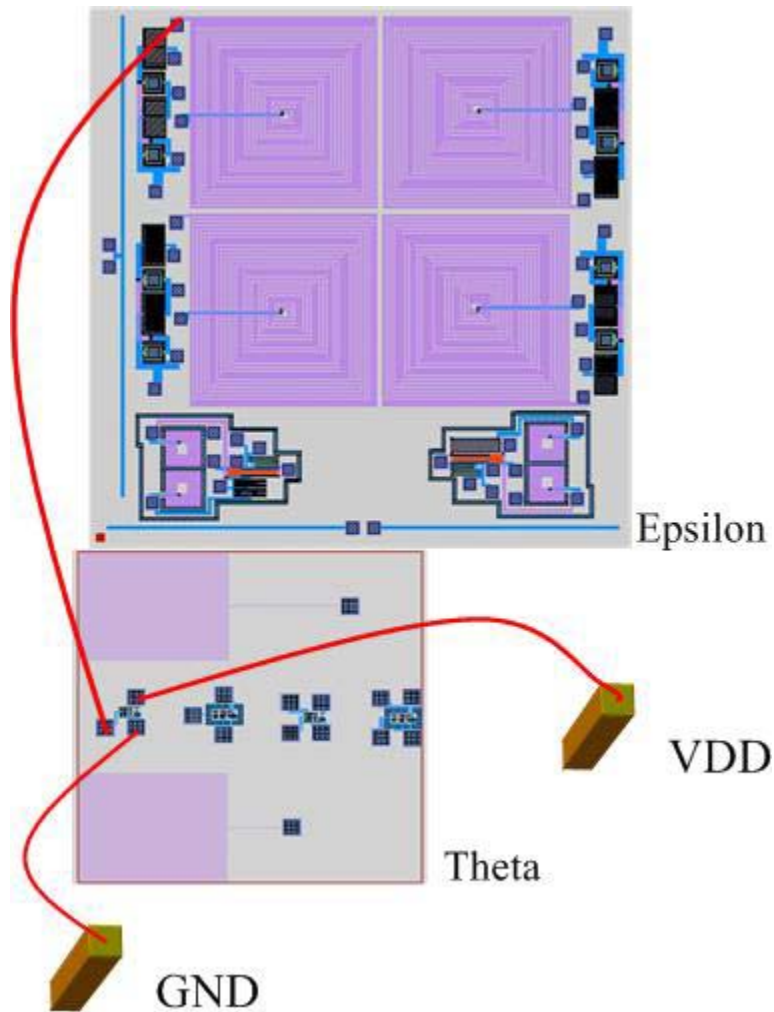


Figure 53. Bonding Diagram of Transmission Experiment

9.2.1.4 Equipment Setup

Power source

A simple DC power source was connected to the test rig using SMA connectors with a Pomona 3073 power adaptor (Figure 45). The power source ranged from zero to six volts. The power source sitting to the left of the network analyzer can be seen in figure 54.

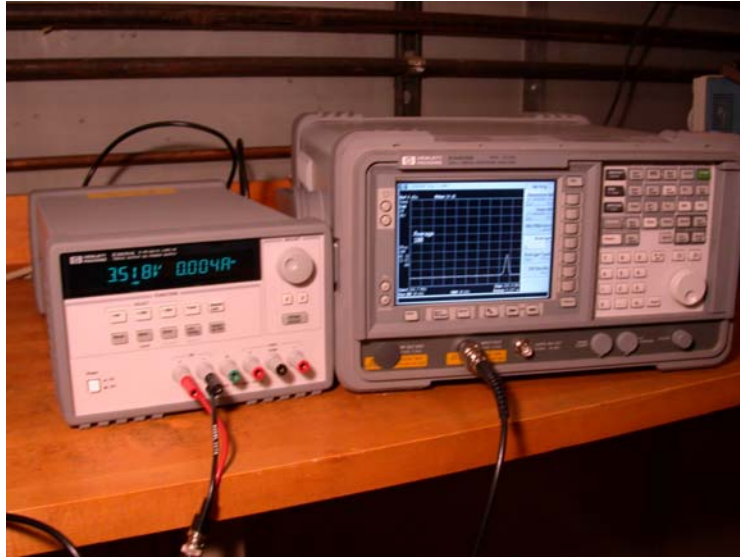


Figure 54. Test Equipment

Receiving antenna

The receiving antenna, MFB-9300, was an omnidirectional fiberglass base station antenna made by Maxrad. It was tuned for 896-940 MHz. The half wave antenna is DC grounded, with a vertical polarization and a nominal impedance of 50 Ohms. The antenna can be seen in figure 55.

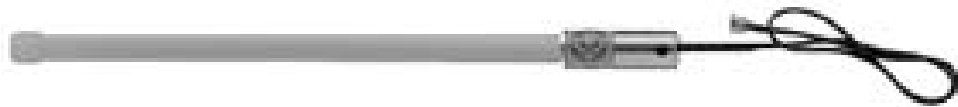


Figure 55. Maxrad 900 MHz antenna

Network analyzer

An E4403B Agilent Spectrum Analyzer was used to detect the transmitted frequency. The analyzer's frequency range is 9 kHz to 3 GHz. The VCOs range was around 500 MHz. A small

test window of 10 MHz was used to find the initial signal. Figure 56 shows the network analyzer with the antenna and the test rig.

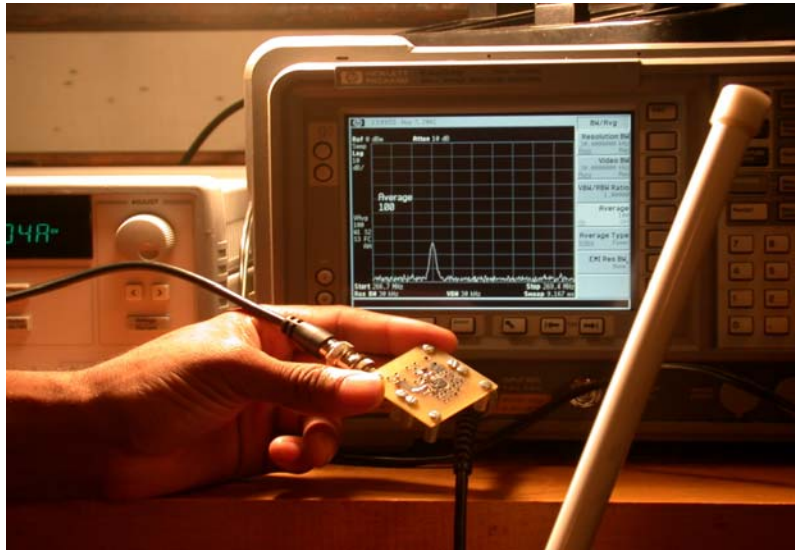


Figure 56. Spectrum Analyzer, Test Rig and Receiving Antenna

Test environment

The low wattage transmission required an RF shielded room to be used for the initial testing. The shielded room is approximately 25 x 15 feet, and can be sealed from the inside. The transmission was possible in an uncontrolled environment, but must be averaged to eliminate noise. The disadvantage of using averaging is the voltage cannot be rapidly changed. If the voltage is rapidly changed the results may be delayed or missed on the spectrum analyzer.

Equipment Setup

The DC power supply was connected to the test rig by the coaxial cable. The VCO then transmits the signal to the receiving antenna. The receiving antenna was connected to the spectrum analyzer by another coaxial cable. The distance of the transmission was between 6

inches and 15 feet. The limitation of the transmission distance was the length of the connected coaxial cables. The test setup can be more clearly visualized in figure 57.

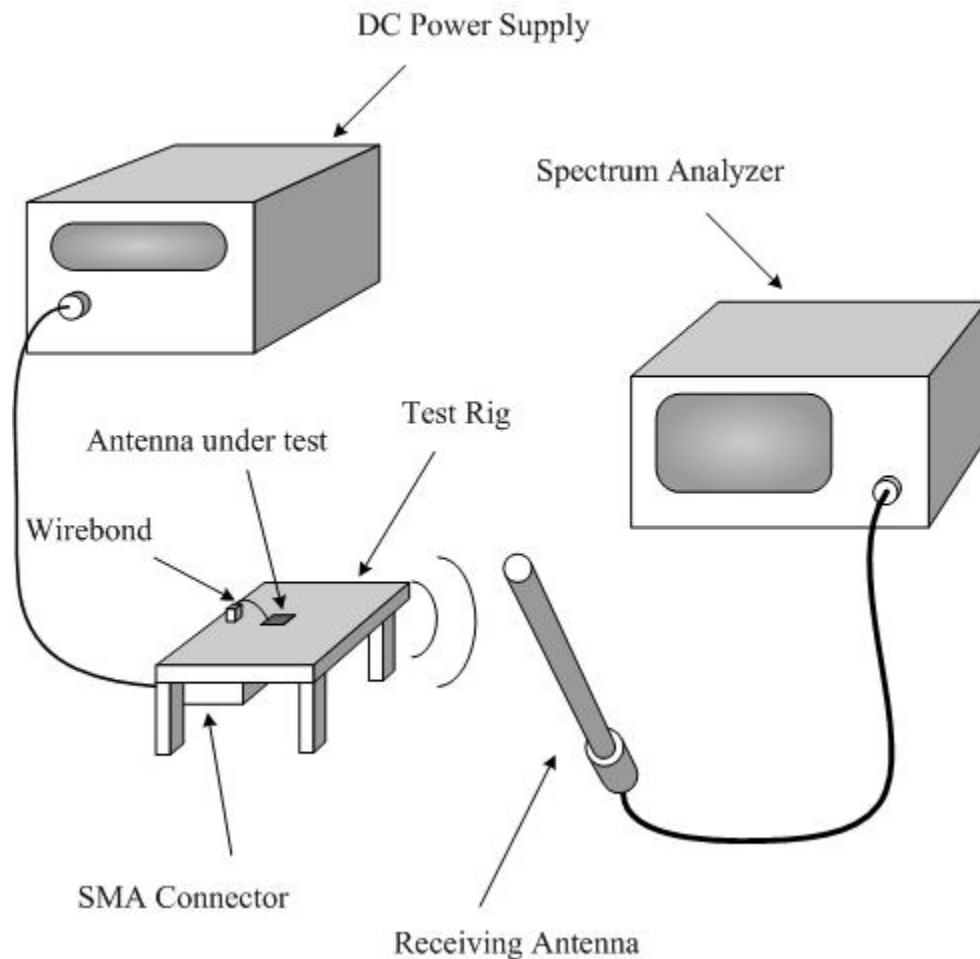


Figure 57. Transmit I Test Setup

9.2.2 Results

The transmitted frequencies were similar to the previously tested non-transmitted frequencies. The signal strengths were obviously lower, but the frequencies were extremely close as displayed in table 4 and graphed in figure 58. The average delta was 2.6 MHz. With a frequency range of

over 400 MHz the average delta is negligible, making this experiment a success. The actual signal can be seen on screen shots from the spectrum analyzer in figures 72-75.

Table 4. Transmitted Results Compared to the Non-Transmitted Results

<u>Voltage</u>	<u>Non-Trans Freq.</u>	<u>Trans Freq.</u>	<u>Delta</u>
3.0	209.1	208	1.1
3.5	268.9	267	1.9
4.0	326.0	323	3.0
4.5	380.2	377	3.2
5.0	431.2	428	3.2
5.5	478.9	476	2.9
6.0	523.8	521	2.8

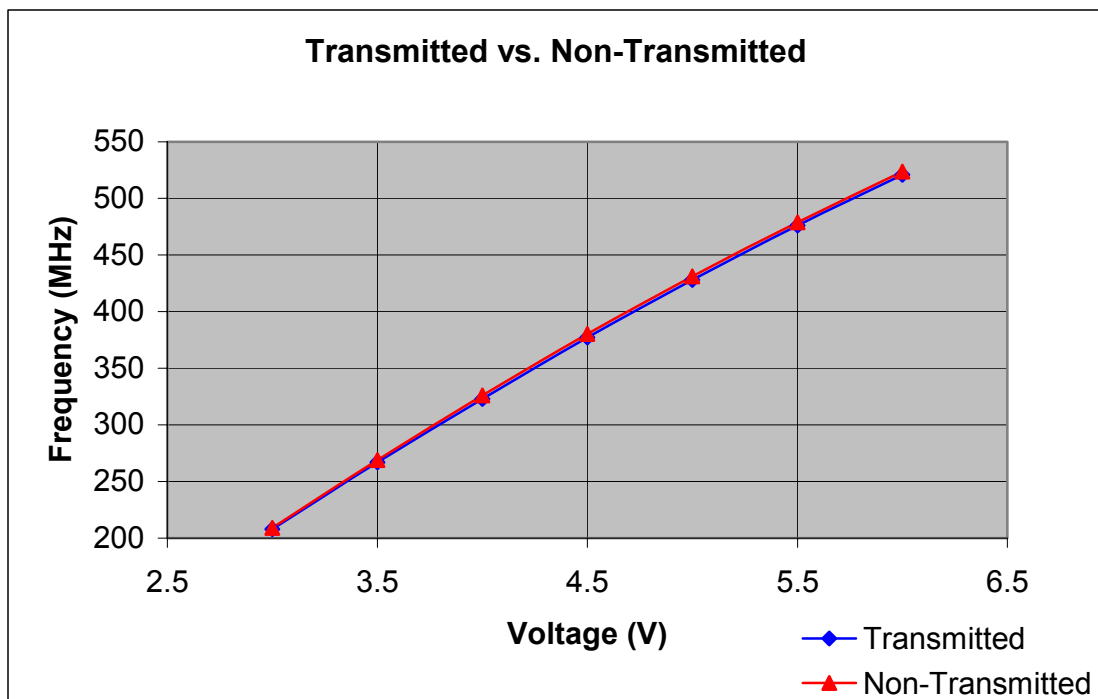


Figure 58. Transmitted I Compared to Non-Transmitted Results

9.3 TRANSMISSION II EXPERIMENT

The purpose of the second transmission experiment was to transmit the VCOs frequency by powering the VCO from harvested RF energy, which was converted to DC energy by the voltage doubler. This is intended to prove both the antennas' harvesting and transmitting ability. This would also prove that a VCO used as a transducer can be used as a method of testing on-chip antennas.

9.3.1 Description

9.3.1.1 Objective

The objective of the experiment was to accurately measure the amount of power being transmitted without touching the chip. The results would then be compared to the results from the previous two experiments. This would prove the antenna's transmitting and harvesting abilities and confirm consistent voltage verse frequency of the VCO from test to test.

9.3.1.2 What was accomplished

The experiment was unsuccessful. A single chip was fabricated and made that contained an energy harvesting antenna, which is connected to a voltage doubler, which powers a VCO, who's signal is transmitted by a spiral, delta antenna. The name of the chip was Iota (figure 59). There were two major factors contributing in Iota not functioning correctly. Both were based off of limitations with the fabrication. Due to limited area available on the chip the largest two antennas that would fit on the chip were tuned to 915 MHz and 2.45 GHz. The 915 MHz was used for the energy harvesting, and the 2.45 GHz was used for transmitting. The RF energy was focused at the chip at 915 MHz, but the transmitting frequency of the VCO was in the 100-600 MHz range. The 2.45 GHz antenna was not a good antenna for this situation.

The second reason for the unsuccessful chip was process limitations. The older technology limits the efficiency of the VCO. The 5 volts required to switch the transistor is too demanding. The VCO was designed to consume very little power, but the high voltage is still necessary to switch the transistor. A more recent process would be necessary to complete this experiment.

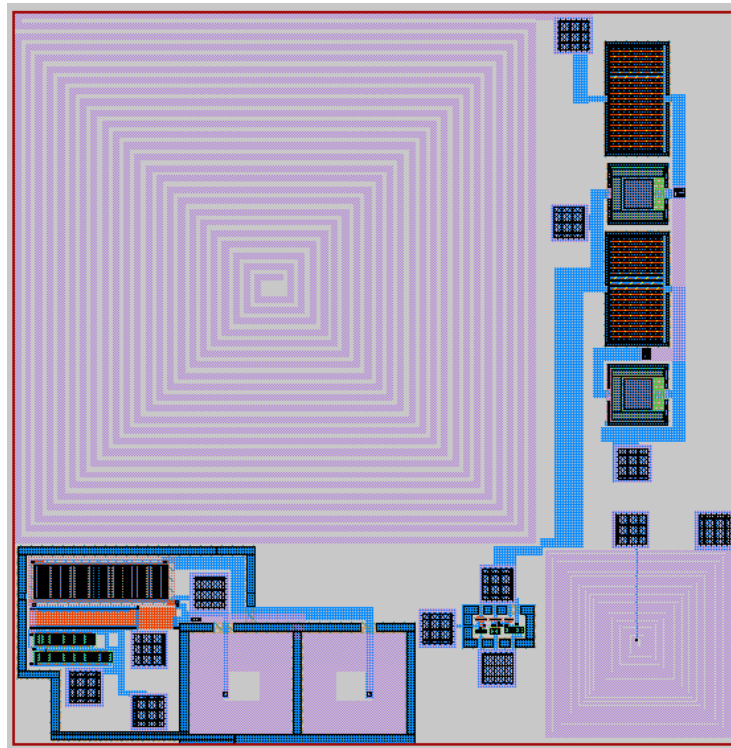


Figure 59. Iota Chip

9.3.1.3 Test Rig Setup

Chip layouts

The Iota chip was used in this experiment. It contains an energy harvesting antenna in the top left, a voltage doubler in the top right, LC VCO in the bottom left, a current starved VCO in the bottom middle, and a 2.45 GHz transmitting antenna on the bottom right. The LC VCO was not used in this experiment. The harvesting antenna was connected to the voltage doubler which was

connected to the VCO. The VCO and the transmitting antenna were not connected. They were left unconnected so it could be used in other experiments also.

Test rig

The test rig was also made of FR4 PCB with copper traces. The chip was attached to the test rig using conductive epoxy. The purpose of attaching the chip was to prevent losing the chip, and to attach the chips ground/substrate to something.

Wire bonds

There was only one wire bond that was necessary, which was from the output of the VCO to the input of the transmitting antenna. No wire bonds to the test rig were necessary. Figure 60 shows the bond on the Iota chip.

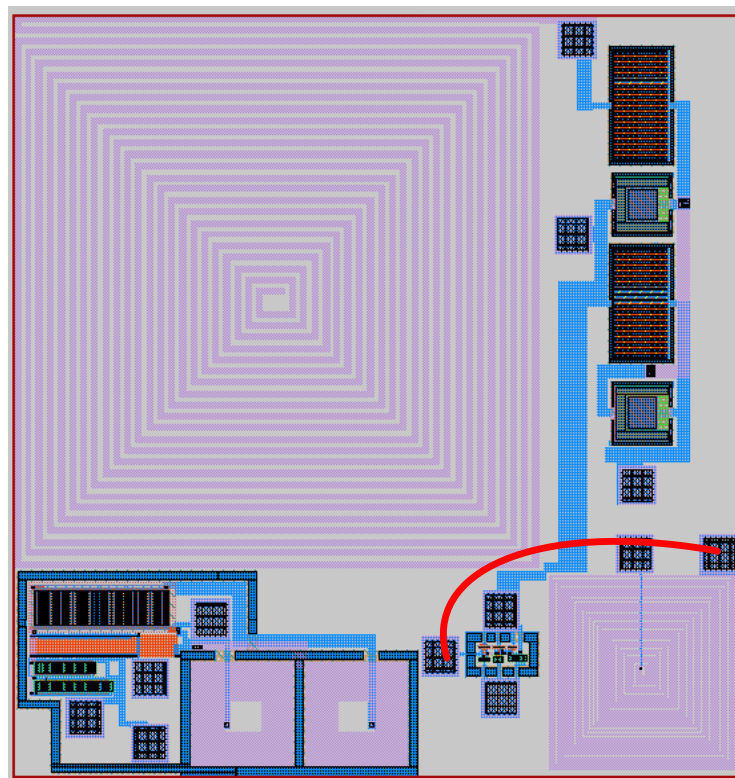


Figure 60. Bonding Diagram of Transmission II Experiment

Equipment Setup

The test required that an RF source is used. To create the RF source to power the chip a signal generator transmitting a sinusoidal wave was connected an RF amplifier. The amplifier boosts the generator's 20mW signal 10W. That is then transmitted by a Maxrad 900 antenna toward the Iota chip. The Iota chip then transmitters the signal to another Maxrad 900 antenna, which is connected to the spectrum analyzer. The test setup can be more clearly visualized in figure 61.

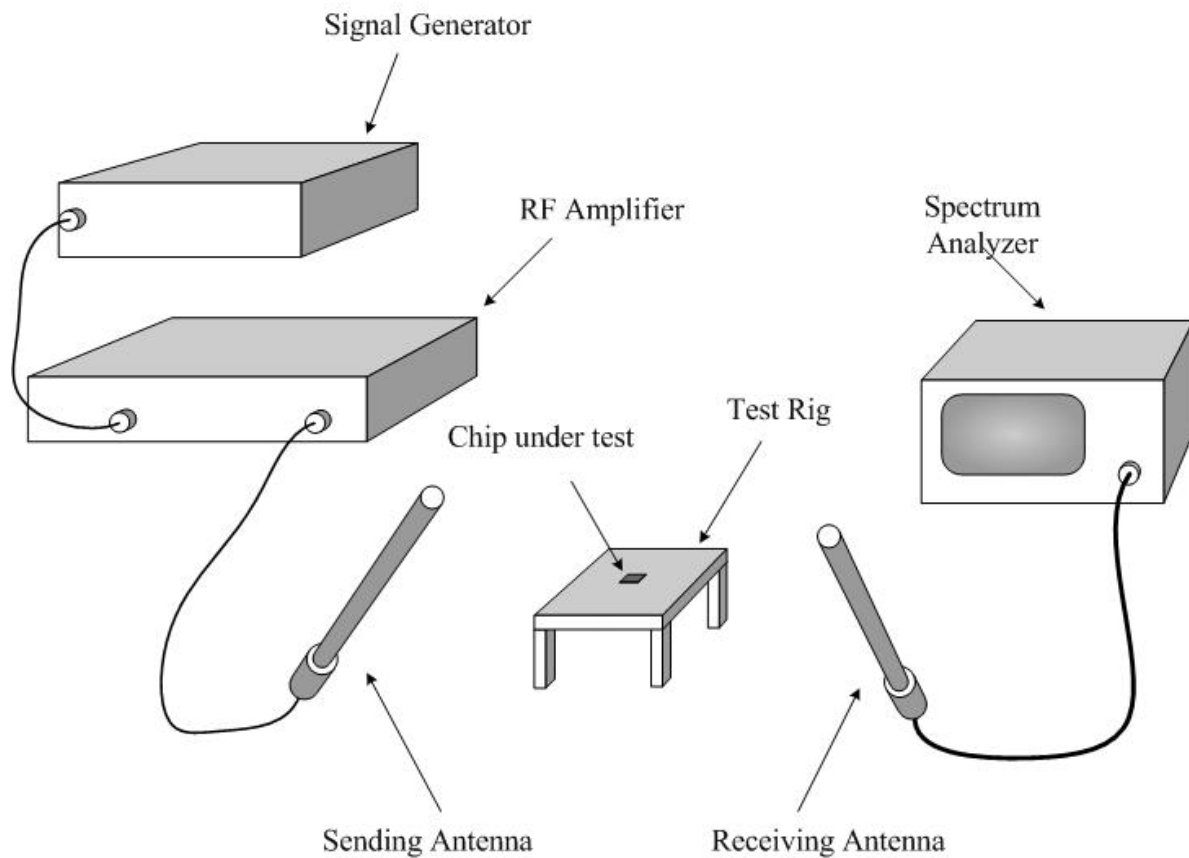


Figure 61. Transmitting II Test Setup

10.0 CONCLUSION

The conclusion of the experimental findings is that using VCOs to test the efficiency of an antenna is possible. The method provides an accurate means of testing energy harvesting antennas. This method does however require you to the VCO on the chip with the antennas under test. This may be expensive, especially because cheaper processes cannot be used as explained earlier. The VCO can be bonded to the antennas, but this could affect the efficiency of the antenna.

A problem that could be encountered using this method would be that the CMOS process variation can change a VCO's performance. The change of performance cannot be measured independently from the antenna to which it is connected. The results could contain some slight errors. The margin of error would not be too great due to the possible change versus the very large tuning range. If the VCO is designed with a small tuning range this could greatly affect your results.

Future research efforts could go into analyzing the thermal behaviors of the VCOs. The results from all VCOs will change slightly as the temperature of the chip increases. If the thermal qualities of the VCO are studied more closely they could be predicted and a more accurate analysis of the antenna under test could be achieved.

11.0 CONTRBUTIONS

This research has contributed the following items to the way of science and engineering of a VCO.

1. Identified and categorized the VCOs into three different types, LC, non LC, and special components for use as an embedded wireless diagnostic measurement and communications system.
2. Compiled the necessary characteristics of a VCO to be used as identified earlier in energy harvesting applications. The compiled items are as follows: definition, multiple topologies, uses, and currently researched efforts of a VCO.
3. Identify and document an appropriate basis topology and achieved better results. The current starved topology shown in figure 12 was chosen for the experiments. In order to reduce the amount of power consumed the buffer on the output was changed to two inverters. This change reduced not only power, but also reduced the circuit size.
4. Demonstrated the advantage of tying the supply voltage and the control voltage together. This greatly increased the tuning range and made it possible to use only one voltage source.
5. Designed, laid-out, and fabricated two VCOs with different styles (analog and digital) for the sake of comparison. The two styles yielded different results, which are summarized and reported.
6. Developed setup and executed a method of testing the two different VCOs using the data from the tests as a reference for future tests.

7. Developed, setup, and executed a method of testing the transmitting antenna. The test results were then compared to the previously documented results.
8. Developed an additional method to test an energy harvesting antenna.

APPENDIX A

VCO Comparison Test

11.1 VCO 1 Results

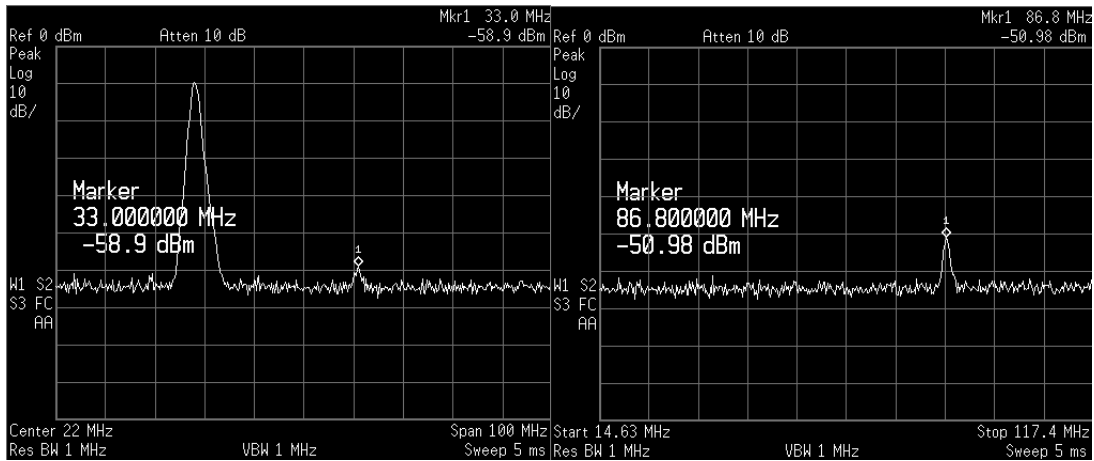


Figure 62. VCO 1 Analyzer Results: 1.5 Volts and 2.0 Volts

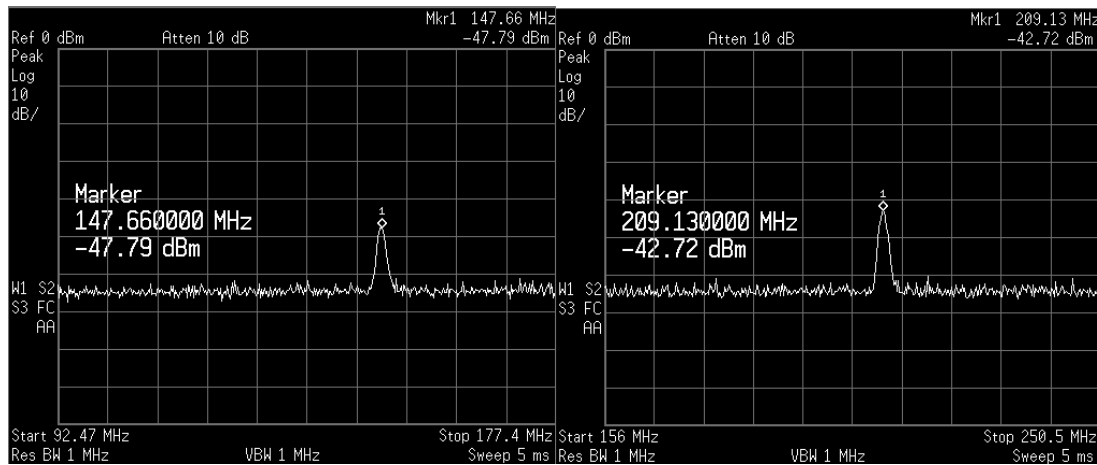


Figure 63. VCO 1 Analyzer Results: 2.5 Volts and 3 Volts

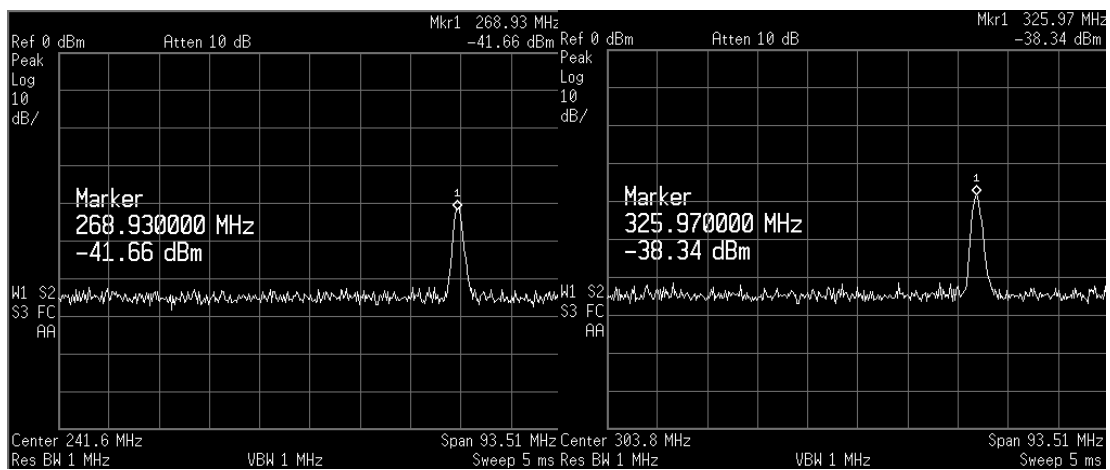


Figure 64. VCO 1 Analyzer Results: 3.5 Volts and 4 Volts

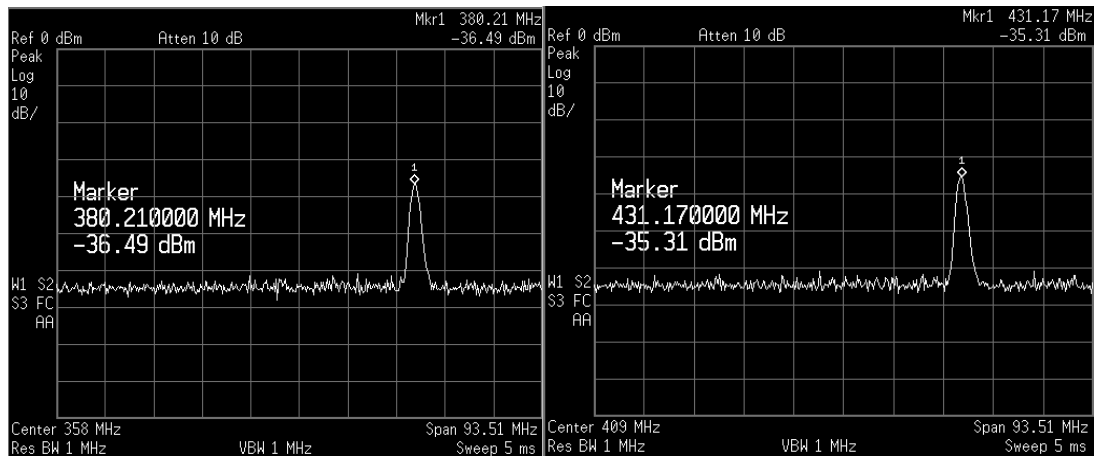


Figure 65. VCO 1 Analyzer Results: 4.5 Volts and 5 Volts

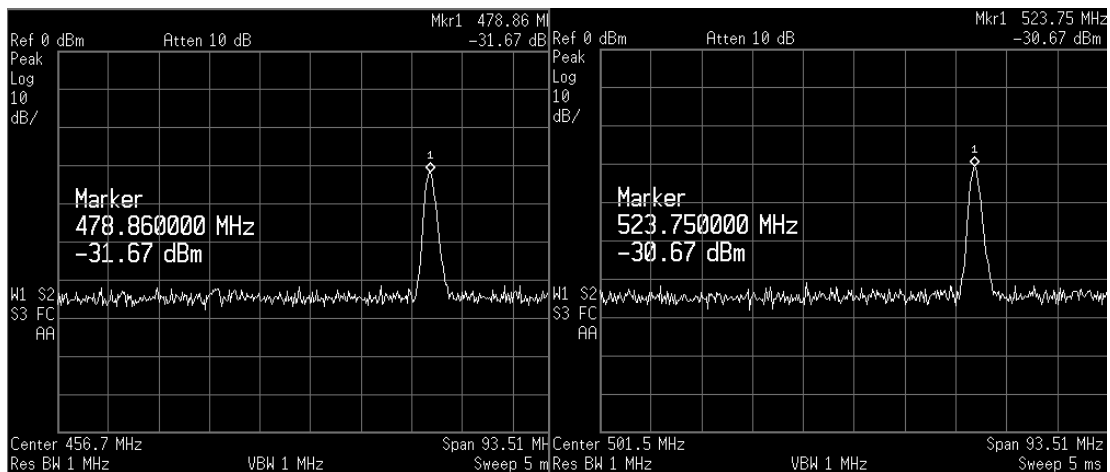


Figure 66. VCO 1 Analyzer Results: 5.5 Volts and 6 Volts

11.2 VCO 2 Results

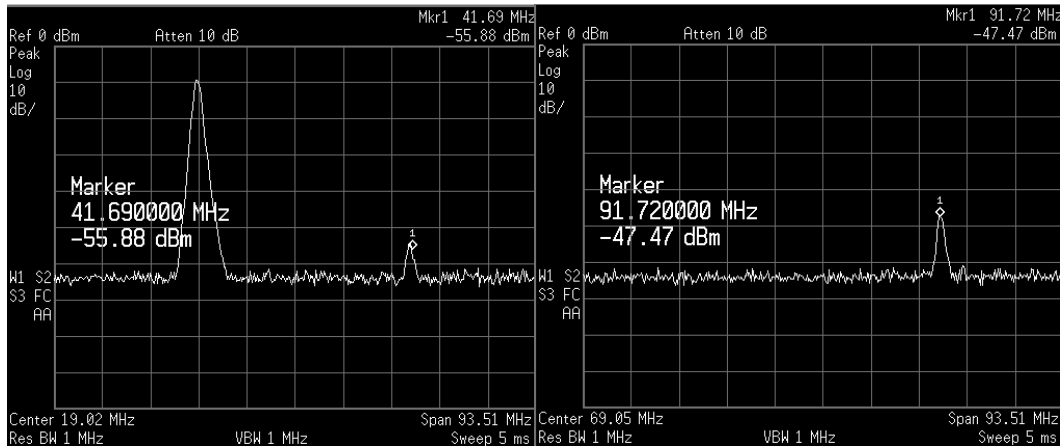


Figure 67. VCO 2 Analyzer Results: 1.5 Volts and 2 Volts

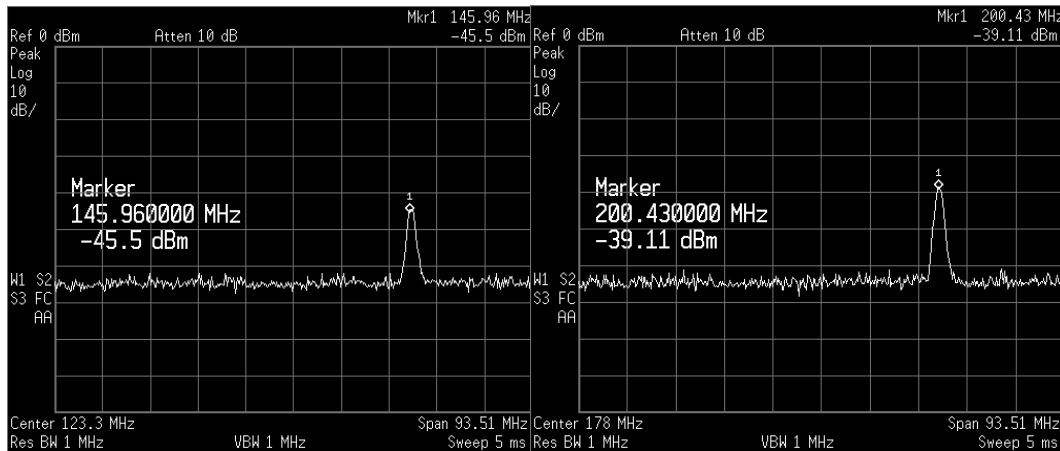


Figure 68. VCO 2 Analyzer Results: 2.5 Volts and 3 Volts

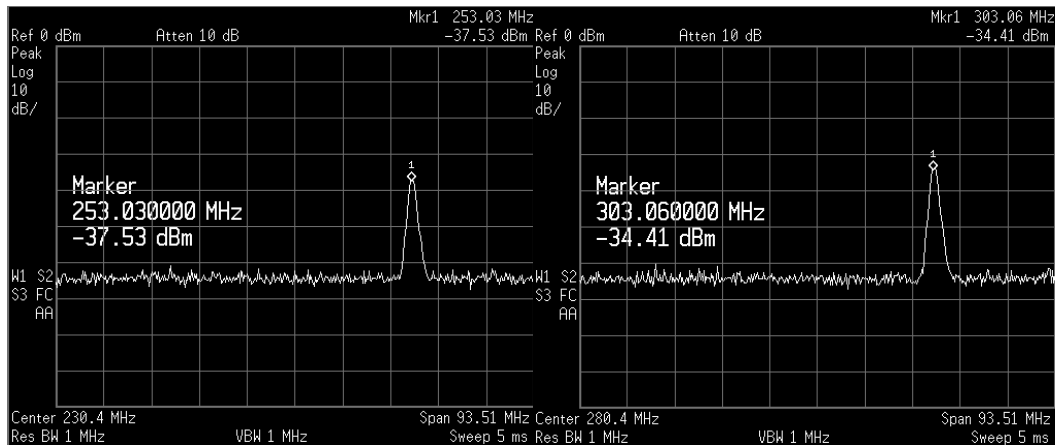


Figure 69. VCO 2 Analyzer Results: 3.5 Volts and 4 Volts

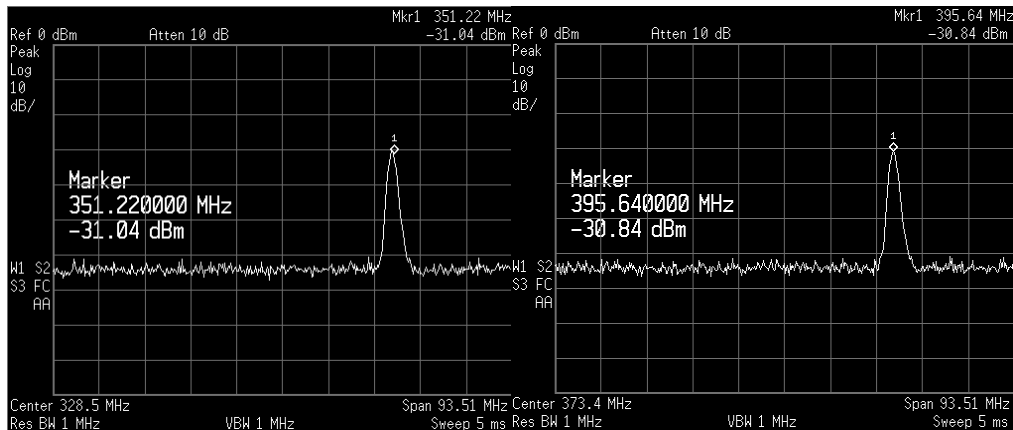


Figure 70. VCO 2 Analyzer Results: 4.5 Volts and 5 Volts

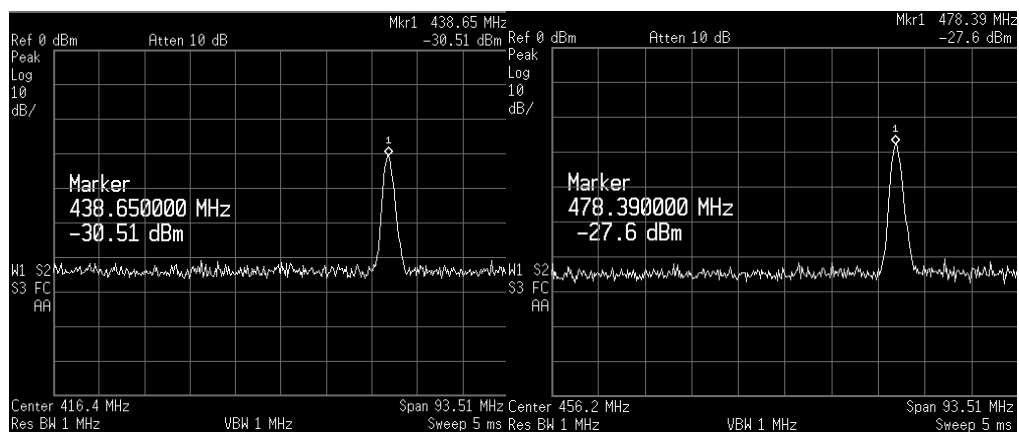


Figure 71. VCO 2 Analyzer Results: 5.5 Volts and 6 Volts

APENDIX B

Transmission Experiment

11.3 Transmission Results

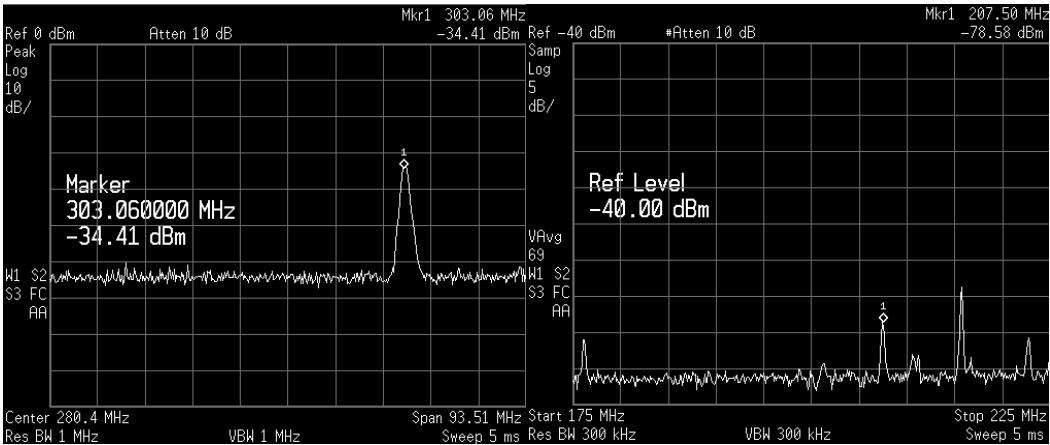


Figure 72. Transmitted Analyzer Results: 2.5 Volts and 3 Volts

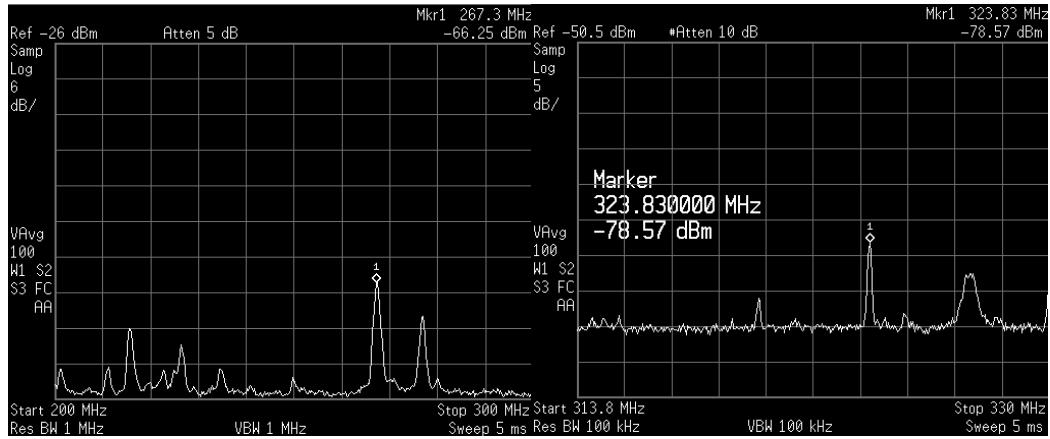


Figure 73. Transmitted Analyzer Results: 3.5 Volts and 4 Volts

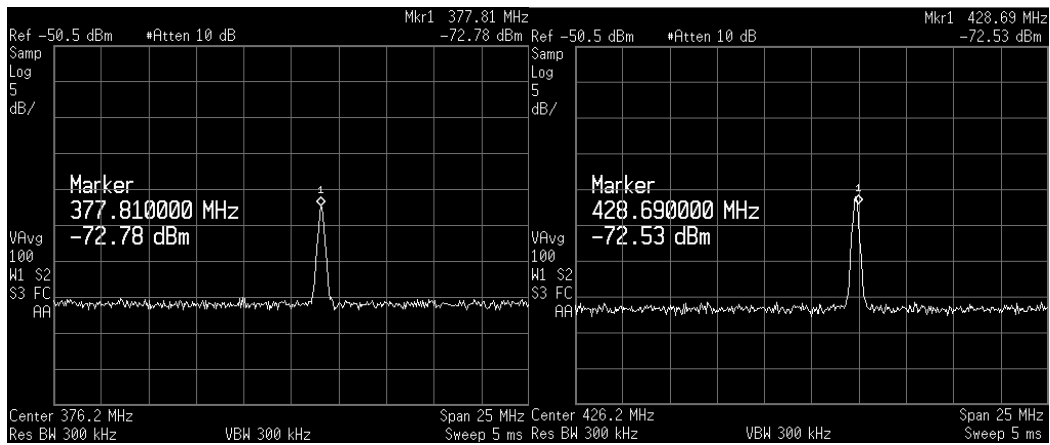


Figure 74. Transmitted Analyzer Results: 4.5 Volts and 5 Volts

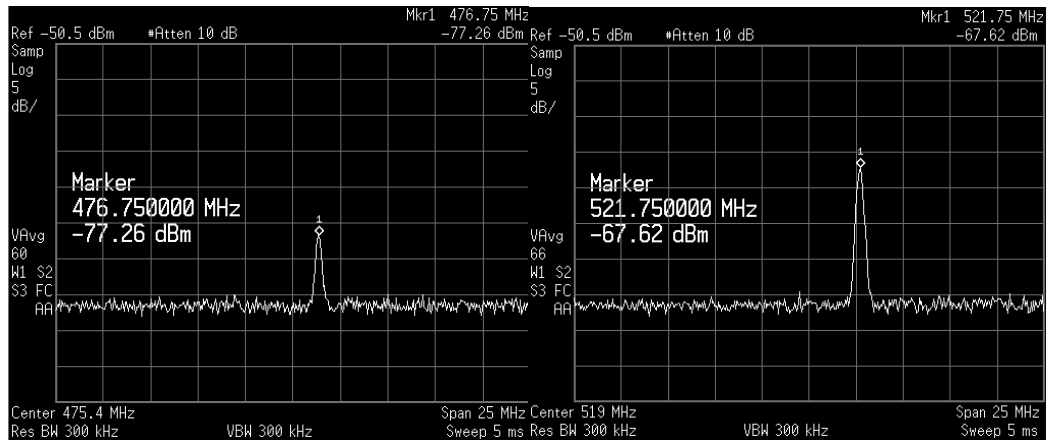


Figure 75. Transmitted Analyzer Results: 5.5 Volts and 6 Volts

BIBLIOGRAPHY

1. Herzel, F.; Pierschel, M.; Weger, P.; Tiebout, M. "Phase Noise in a Differential CMOS Voltage-Controlled Oscillator for RF Applications." *IEEE Transactions on Circuits and Systems - II, Volume: 47 Issue 1* January 2000: 11–15.
2. Kato, K.; Sase, T.; Hideo, S.; Ikushima, I.; Kojima S. "A Low-Power 128-MHz VCO for Monolithic PLL IC's." *IEEE Journal of Solid-State Circuits, Volume 23, Number 2* April 1988: 474-479.
3. Razavi, Behzad. *Design of Analog CMOS Intergrated Circuits*. New York: McGraw-Hill, 2001.
4. Lee, Thomas. *The Design of CMOS Radio-Frequency Integrated Circuits*. New York: Cambridge University Press, 1998.
5. Dec, A.; Suyama K. "A 1.9-GHz CMOS VCO with Micromachined Electromechanically Tunable Capacitors." *IEEE Journal of Solid-State Circuits, Volume 35, Number 8* August 2000: 1231-1237.
6. Craninckx, J.; M. Steyaert, and H. Miyakawa. "A Fully Integrated Spiral-LC CMOS VCO Set with Prescaler for GSM and DCS-1800 Systems." *IEEE 1997 Custom Integrated Circuits Conference* 1997: 736-744.
7. Svelto, F., S. Deantoni, R. Castello. "A 1.3 GHz Low-Phase Noise Fully Tunable CMOS LC VCO." *IEEE Journal on Solid State Circuits, Volume 35, Number 3* March 2000.
8. Andreani, P., S. Mattisson. "On the Use of MOS Varactor in RF VCO's." *IEEE Journal of Solid-State Circuits, Volume 35, Number 6* June 2000.
9. Thamsirianunt, M, A. Kwasniewski. "CMOS VCO for PLL Frequency Synthesis in GHz Digital Mobile Radio Communications." *IEEE Journal of Solid-State Circuits, Volume 32, Number 10* October 1997.
10. Gottlieb, Irving. *Practical Oscillator Handbook*. Oxford: Newnes, 1997

11. Gray, Paul, P. J. Hurst, S. H. Lewis, and R.G. Meyer. *Analysis and Design of Analog Integrated Circuits*. John Willy & Sons, Inc. 2001.
12. Baker, R. J., H. W. Li, and D. E. Boyce. *CMOS Circuit Design, Layout, and Simulation*. IEEE Press. 1998.
13. Apparatus for Energizing a Remote Station and Related Method, U.S. Patent No. 6,289,237, University of Pittsburgh. Mickle, Marlin H., K. W. Wells, R. G. Hoelzeman. September 11, 2001 (40 claims).
14. Apparatus for Energizing a Remote Station and Related Method, Continuation In Part, Serial No. 09/951,032. University of Pittsburgh. Mickle, Marlin H., L. Mats, L. Neureuter, M. Mi, D. Gorodetsky, C. Taylor and C. Emahiser. Filed September 10, 2001 (55 claims).
15. <http://www.radiolab.com.au>
16. <http://www.saronix.com>
17. Ahrens, T. I., and T. H. Lee. "A 1.4-GHz 3-mW CMOS LC low phase noise VCO using tapped bond wire inductances." *Low Power Electronics and Design, 1998*, 1998: pages 16-19.
18. Soga, Shuji, Y. Hiroshige, A. Dobashi, M. Okumura, and T. Kusuzaki. "Products Lifecycle Management System Using Radio Frequency Identification Technology."
19. <http://www.speedpass.com>
20. <http://www.ezpass.com>
21. Razavi, Behzad. "A Study of Phase Noise in CMOS Oscillators." *IEEE Journal of Solid-State Circuits, Vol. 31, No. 3*, March 1996: pages 331-343.
22. Herzel, Frank, H. Erzgraber and P. Weger. "Integrated CMOS Wideband Oscillator for RF Applications." *IEEE Electronics Letters, Vol. 37, Issue: 6*, 15 March 2001: pages 330-331.
23. Herzel, Frank, H. Erzgraber and N. Ilkov. "A New Approach to Fully Integrated CMOS LC-Oscillators with a Very Large Tuning Range" *Custom Integrated Circuits Conference, 2000. CICC Proceedings of the IEEE 2000*, 2000: pages 573-576.
24. Hung, Chih-Ming, L. Shi, I. Languado, and K. K. O. "A 25.9-GHz Voltage Controlled Oscillator Fabricated in a CMOS process." *VLSI Circuits, 2000. Digest of Technical Papers. 2000 Symposium on*, 2000: pages 100-101.
25. Wilson, William, Un-Ku Moon, K. Lakshmikumar, L. Dai. "A CMOS Self-Calibrating Frequency Synthesizer." *IEEE Journal of Solid-State Circuits, Vol. 35, No. 10*, October 2000: pages 1437-1444.

26. Hung, Chih-Ming, B. Floyd, N. Park, and K. K. O. "Fully Integrated 5.35-GHz CMOS VCOs and Prescalers." *IEEE Transactions on Microwave Theory and Techniques*, Vol. 49, No. 1, January 2002: pages 17-22.
27. Andreani, Pietro. "A 1.8-GHz Monolithic CMOS VCO Tuned by an Inductive Varactor." *Circuits and Systems, 2001. ISCAS 2001. The 2001 IEEE International Symposium on*, Vol. 4, 2001: pages 714-717.
28. Andreani, Pietro and S. Mattisson. "A 2.4-GHz CMOS Monolithic VCO Based on an MOS Varactor."
29. Andreani, Pietro. "A 1.8-GHz CMOS VCO Tuned by an Accumulation-Mode Varactor." *Circuits and Systems, 2001. ISCAS 2001. The 2001 IEEE International Symposium on*, Vol. 4, 2001: pages 714-717.
30. Pott, V., and others. "The Suspended-Gate MOSFET (SG-MOSFET): A Modeling Outlook for the Design of RF MEMS Switches and Tunable Capacitors."
31. Dec, A.; Suyama K. "RF Micromachined Varactors with Wide Tuning Range." *Radio Frequency Integrated Circuits Symposium, 1998 IEEE*. 7-9 Jun 1998: pages 309-312.
32. De Ranter, C. R. C., M. S. J. Steyaert. "A 0.25 μm CMOS 17 GHz VCO." *Solid-State Circuits Conference, 2001. Digest of Technical Papers. ISSCC. 2001 IEEE International*. 2001: pages 370-371, 466.
34. <http://www.mosis.org>